

TOPICAL REVIEW • OPEN ACCESS

Recent advances in wave-driven triboelectric nanogenerators: from manufacturing to applications

To cite this article: Chuanqing Zhu *et al* 2024 *Int. J. Extrem. Manuf.* **6** 062009

View the [article online](#) for updates and enhancements.

You may also like

- [Recent advances in nature inspired triboelectric nanogenerators for self-powered systems](#)
Baosen Zhang, Yunchong Jiang, Tianci Ren *et al.*
- [Waterwheel-inspired high-performance hybrid electromagnetic-triboelectric nanogenerators based on fluid pipeline energy harvesting for power supply systems and data monitoring](#)
Mengying Lian, Jiaxin Sun, Dawei Jiang *et al.*
- [From contact electrification to triboelectric nanogenerators](#)
Zhong Lin Wang

Topical Review

Recent advances in wave-driven triboelectric nanogenerators: from manufacturing to applications

Chuanqing Zhu¹ , Cheng Xiang¹, Mengwei Wu², Chengnuo Yu¹, Shu Dai³, Qijun Sun⁴ , Tongming Zhou^{5,*}, Hao Wang^{1,*} and Minyi Xu^{1,*} 

¹ Marine Engineering College, Dalian Maritime University, Dalian, People's Republic of China

² College of Engineering, Peking University, Beijing, People's Republic of China

³ Shanghai Investigation, Design & Research Institute Co., Ltd, Shanghai, People's Republic of China

⁴ Beijing Institute of Nanoenergy and Nanosystems, CAS, Beijing, People's Republic of China

⁵ Civil, Environmental and Mining Engineering, The University of Western Australia, Perth, Australia

E-mail: tongming.zhou@uwa.edu.au, hao8901@dltmu.edu.cn and xuminyi@dltmu.edu.cn

Received 1 March 2024, revised 12 May 2024

Accepted for publication 14 September 2024

Published 26 September 2024



Abstract

The ocean is the largest reservoir of renewable energy on earth, in which wave energy occupies an important position due to its high energy density and extensive distribution. As a cutting-edge technology, wave-driven triboelectric nanogenerators (W-TENGs) demonstrate substantial potential for ocean energy conversion and utilization. This paper provides a comprehensive review of W-TENGs, from materials manufacturing and structural fabrications to marine applications. It highlights the versatility in materials selection for W-TENGs and the potential for unique treatments to enhance output performance. With the development of materials science, researchers can manufacture materials with various properties as needed. The structural design and fabrication of W-TENGs is the pillar of converting wave energy to electrical energy. The flexible combination of TENG's multiple working modes and advanced manufacturing methods make W-TENGs' structures rich and diverse. Advanced technologies, such as three-dimensional printing, make manufacturing and upgrading W-TENGs more convenient and efficient. This paper summarizes their structures and elucidates their features and manufacturing processes. It should be noted that all efforts made in materials and structures are aimed at W-TENGs, having a bright application prospect. The latest studies on W-TENGs for effective application in the marine field are reviewed, and their feasibility and practical value are evaluated. Finally, based on a systematic review, the existing challenges at this stage are pointed out. More importantly, strategies to address these challenges and directions for future research

* Authors to whom any correspondence should be addressed.



Original content from this work may be used under the terms of the [Creative Commons Attribution 4.0 licence](#). Any further distribution of this work must maintain attribution to the author(s) and the title of the work, journal citation and DOI.

efforts are also discussed. This review aims to clarify the recent advances in standardization and scale-up of W-TENGs to promote richer innovation and practice in the future.

Keywords: wave energy, triboelectric nanogenerator, materials manufacturing, structural fabrication, marine application

1. Introduction

The rapid advancement of the global economy has led to an escalating demand for energy [1–4]. The prevalent reliance on traditional fossil fuels for energy causes serious environmental and social problems [5–8], including extreme weather events [9], air pollution [10] and compromised energy security [11]. In this context, it becomes particularly urgent to seek renewable energy as a new energy pillar [12–15]. As the largest natural resource pool on earth, the ocean contains abundant renewable energy [16]. The development and utilization of ocean energy are expected to solve the current dilemma and achieve a green transformation of the global economy [17–19].

Wave energy is particularly prominent among all ocean energy sources, mainly due to its high energy density, continuous energy supply and extensive distribution [20–22]. Moreover, the development of wave energy harnessing facilities has less impact on the marine environment and has good compatibility with the marine ecosystem [23]. However, the process of effectively collecting and converting wave energy into electrical energy still presents numerous challenges. These challenges mainly stem from the instability of wave energy itself and the harsh ocean environment [24, 25]. Currently, in the field of wave energy collection, electromagnetic generators (EMGs) are commonly applied due to their established designs and high power output [26–28]. However, their larger size and complexity, as well as the associated installation and maintenance costs, form a considerable barrier in adapting to the complex and changeable marine environment [29]. Therefore, developing efficient, stable, and adaptable wave energy technology is critical in making wave energy a pillar of renewable energy.

In 2012, triboelectric nanogenerators (TENGs) were invented by Fan *et al*, which can directly convert mechanical energy into electrical energy [30]. The emergence of TENGs, with their unique working principle and excellent energy conversion efficiency, has brought new options for effectively utilizing wave energy. Wave-driven TENGs (W-TENGs), as a new type of energy collection device, have the advantages of simple structure, low cost, and good adaptability compared to traditional energy conversion technologies [31]. Particularly in marine environments, W-TENGs show unique benefits and can collect wave energy directly under ultra-low frequencies. The first W-TENG was proposed by Yang *et al* [32] in 2013. It adopted a spherical structure and generated electricity based on the contact–separation of polytetrafluoroethylene (PTFE) and polyamide (PA) films. A closed cylindrical

W-TENG was also developed, and the energy generated could directly light up LED lights or be stored in lithium–ion batteries. Subsequently, various dielectric materials were explored for manufacturing W-TENGs, with their output performance optimized through physical and chemical treatment [33–35]. In 2015, Wang *et al* [36] proposed to adopt rolling balls as the internal motion structure inside the W-TENGs. The instability of the internal ball motion significantly enhanced the adaptability of W-TENGs to the marine environment. Research has shown that the rolling design of W-TENGs could respond more effectively to waves, making it the mainstream structure of W-TENGs [37, 38]. To more effectively collect wave energy in various types and directions, researchers have designed W-TENGs with multiple structures. Chen *et al* [39] carried out a network design of W-TENG units and promoted the use of W-TENGs on a large scale. The study predicts that the vast ocean area will meet existing energy needs if W-TENGs are appropriately deployed. The above works were initially applied in fields such as self-powered ocean nodes. Moreover, the sufficient energy provided by W-TENGs also proves its application prospects in other fields [40, 41]. While realizing the iterative upgrade of W-TENGs, its application fields will also be further expanded [42, 43].

In the past few years, several excellent reviews have elucidated the latest developments related to W-TENGs, providing a comprehensive understanding of various research [44–50]. These reviews have analyzed material processing [51], classified existing structures [52], and summarized applications in some fields [47, 53, 54]. However, they have not offered a macroscopic summary of the entire research process of W-TENGs. In order to enable researchers to understand the progress of the whole field quickly, this review begins with the basic principles and fundamental working models of TENGs and systematically elaborates on the recent advances of W-TENGs. The structure of the paper is shown in figure 1 [39, 55–63]. The research discussed in sections 3–5 is not isolated but inclusive of each other, and closely follows a core. The main idea is to review the development of the technology, from working mechanisms to overall structures and from microscopic processing to macroscopic applications. Firstly, this paper details basic materials manufacturing, including materials selection, contact optimization, chemical treatment, and new materials preparation. Secondly, it explores advanced structural design and fabrication, such as multi-layer, channel, elastic, and rotating structures. Furthermore, the review highlights the potential applications of W-TENGs in the marine environment, such as large-scale energy harvesting, electrochemical production, ocean navigation support, and

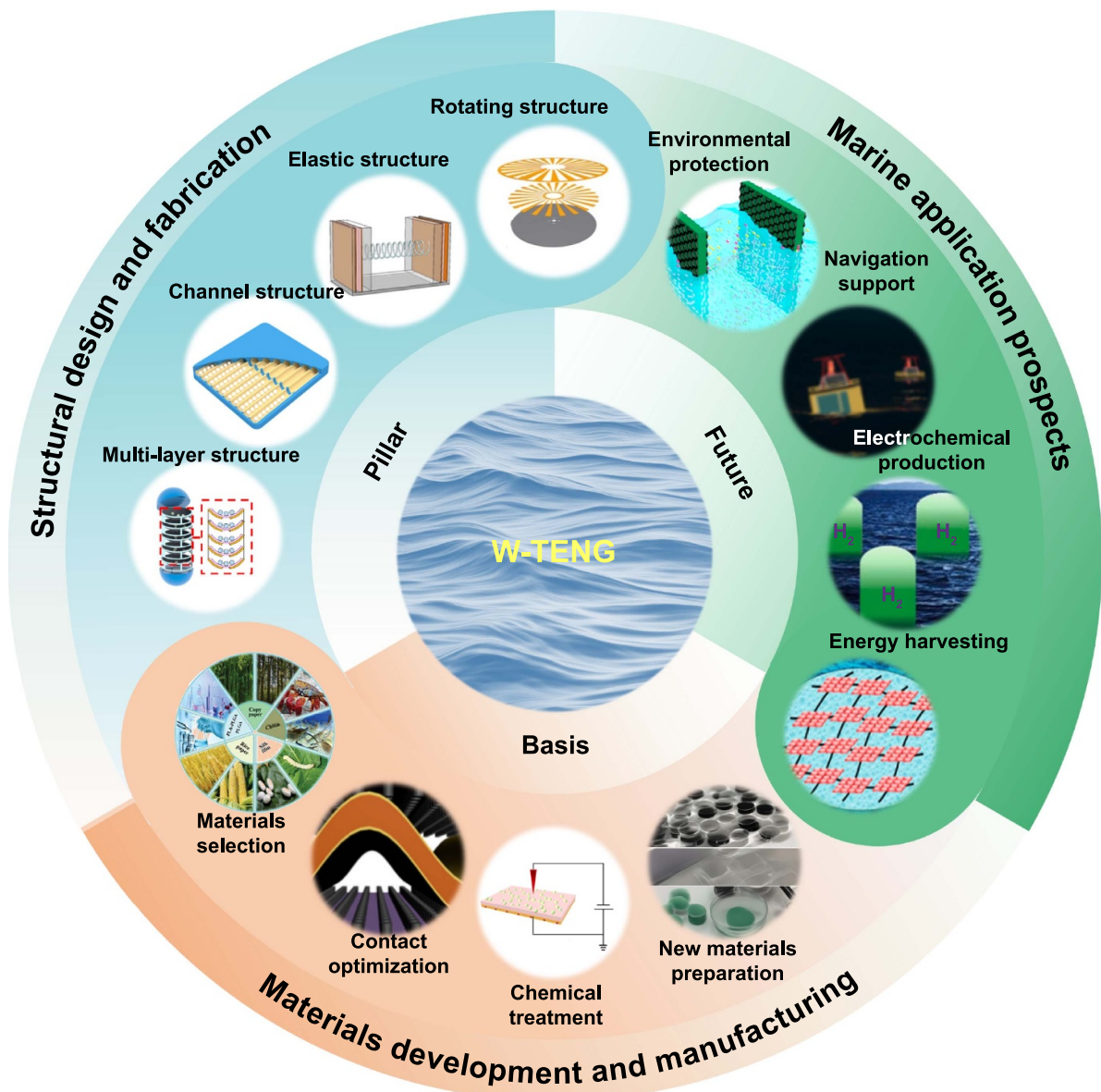


Figure 1. Overview diagram of the W-TENGs from manufacturing to applications. Reprinted (adapted) with permission from [39]. Copyright (2015) American Chemical Society. [55] John Wiley & Sons. © 2020 WILEY-VCH Verlag GmbH & Co. KGaA, Weinheim. Reprinted (adapted) with permission from [56]. Copyright (2014) American Chemical Society. Reprinted from [57]. © 2016 Elsevier Ltd All rights reserved. Reprinted (adapted) with permission from [58]. Copyright (2019) American Chemical Society. Reproduced from [59]. CC BY 4.0. Reprinted from [60], © 2023 Elsevier Ltd All rights reserved. Reprinted from [61], © 2023 Elsevier Ltd All rights reserved. Reprinted from [62], © 2021 Elsevier Ltd All rights reserved. Reprinted from [63], Copyright © 2015 Elsevier Ltd All rights reserved.

environmental protection. Finally, the existing achievements and challenges that W-TENGs face are summarized, and further research on W-TENGs is prospected.

2. Basic principle and fundamental working models

In order to better explain the research progress related to W-TENGs, it is necessary to grasp the foundational principle of the TENGs they employ. This section presents the basic principle and the fundamental working modes of TENGs.

2.1. Basic principle

The power generation principle of TENGs is based on the coupling of triboelectrification (TE) and electrostatic induction [64]. TE means that when two different materials come into contact driven by an external force, they have opposite charges on the surface of the materials. After separation, the potential difference created by electrostatic induction drives electrons to flow in the external circuit, generating the current. Understanding the core principle of power generation hinges on comprehending why materials become charged and

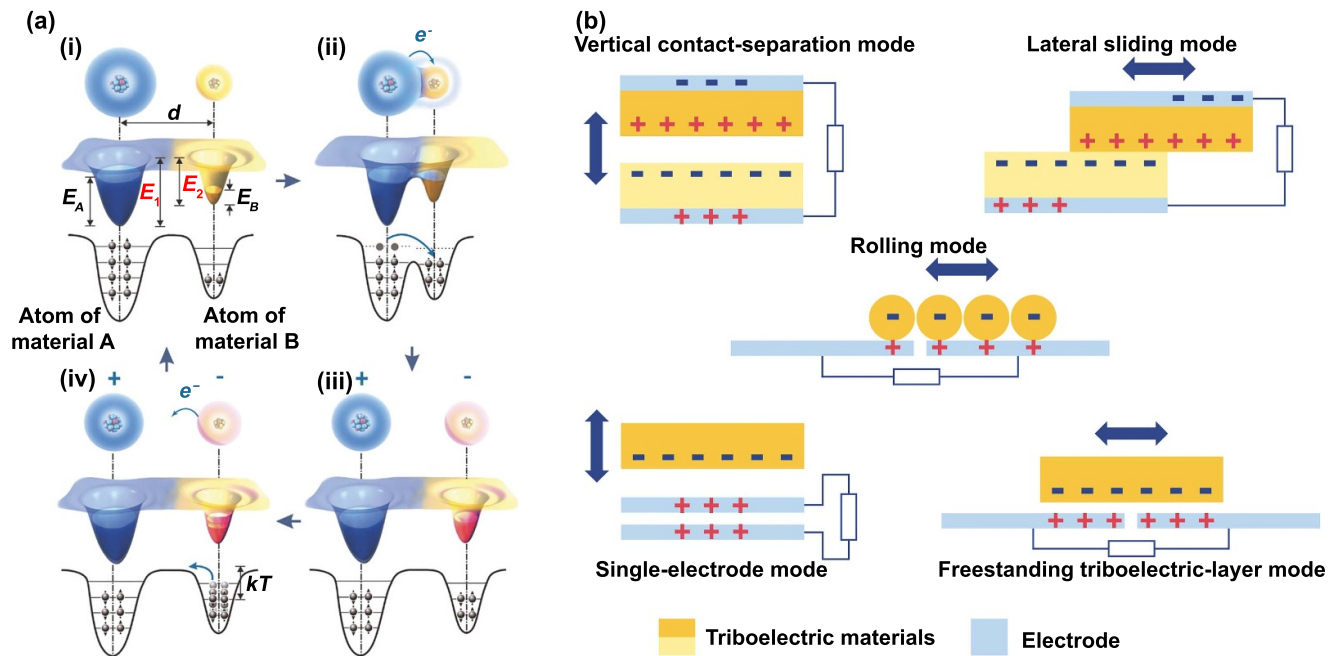


Figure 2. Basic principle and fundamental working models of TENG. (a) The electron cloud/potential model. [66] John Wiley & Sons. © 2018 WILEY-VCH Verlag GmbH & Co. KGaA, Weinheim. (b) Five fundamental working modes.

the mechanisms that allow these charges to persist on the surface without rapid dissipation.

The phenomenon of TE was documented 2 600 years ago, but a clear and unified scientific understanding is lacking [65]. The scientific term for TE is contact electrification (CE), which refers to the production of charges due to physical contact. To explain all types of TE in general materials, Wang *et al* [65–67] proposed an electron cloud/potential model based on fundamental electron cloud interactions.

The spatially localized electrons within specific atoms or molecules, and occupying particular atomic or molecular orbitals can form an electron cloud. As shown in figure 2(a-i), a potential well in which the outer-shell electrons are loosely bounded can represent an atom, with d denoting the distance between electron clouds. The energy levels occupied by electrons in the atoms of materials *A* and *B* are E_A and E_B , and the potential energies required to escape from the surfaces of materials *A* and *B* are E_1 and E_2 . E_A and E_B are smaller than E_1 and E_2 , respectively. Before contact at the atomic level, the electron clouds of the two materials remain separated due to the local trapping effect of the potential well. The potential well binds the electrons tightly in specific orbitals, and the electrons cannot transfer. When materials *A* and *B* come into contact, the intense electron clouds between the two atoms overlap under the action of stress and form an ionic bond or a covalent bond. The original single potential well becomes an asymmetric double-well potential, and then the electrons can transfer from the atom of material *A* to the atom of material *B* (figure 2(a-ii)). When the materials separate, if the temperature is not high, the potential energy E_2 of material *B* will retain most of the transferred electrons (figure 2(a-iii)). This outlines the basic principle underpinning the contact–separation

mechanism of TENGs, which produces positively charged material *A* and negatively charged material *B*. As the temperature increases, the energy fluctuations of electrons become larger and larger as kT increases. This leads to electrons escaping the potential well and either returning to their original atoms, or being emitted into the atmosphere, as shown in figure 2(a-iv). In general, electron transfer dominates the entire process. At the same time, ion or material transfer may also occur, but this process is minor. This electron transition model is named as the Wang transition for CE, which explains why charges generated by CE can persist on the surface.

2.2. Fundamental working models

TENGs are classified into five fundamental working modes according to different mechanical triggering conditions, as shown in figure 2(b). These include the vertical contact–separation mode, lateral sliding mode, single-electrode mode, freestanding triboelectric-layer mode and rolling mode [44].

Vertical contact–separation mode: this mode involves two distinct triboelectric materials coming into vertical contact and subsequently separating from each other. Upon contact, diverse charges accumulate on the surfaces of both materials. The separation of these materials leads to a charge imbalance, prompting electron flow from one electrode to another via an external circuit to neutralize the accumulated charges.

Lateral sliding mode: this mode is characterized by two materials maintaining contact on a common plane while sliding relative to one another. As they slide, triboelectric charges are generated on the contact surface, inducing an electric current between the electrodes due to the relative movement.

Single-electrode mode: in this mode, the electrode of one triboelectric material is connected to the ground, allowing the other material to move freely. This configuration makes single-electrode mode TENGs particularly suitable for motion detection of non-fixed objects. An electric current is generated when the freely moving triboelectric material contacts the grounded material.

Freestanding triboelectric-layer mode: this mode features a dielectric material that can move freely on the electrodes at both ends. The reciprocating movement of this dielectric material generates induced charges on the electrodes. This mode permits the triboelectric material to move unrestrictedly without directly contacting the electrodes, enabling energy collection from multiple directions while minimizing material wear.

Rolling mode: rolling mode integrates the principles of the first four modes, primarily utilizing the interaction between a rolling triboelectric structure, such as a sphere, and a solid surface to generate charges. This mode enhances the rate of contact–separation, consequently amplifying the output.

Different modes of TENGs can be designed according to various scenarios and forms of mechanical energy. Presently, TENGs have been extensively employed for harvesting wind energy [68–72], current energy [73–75], and wave energy [76–78], among others [79–83]. The vast array of triboelectric materials available for selection further broadens the design possibilities of TENGs, making research in this domain increasingly diverse and dynamic.

3. Materials development and manufacturing

The core of TENGs involves contact and separation between two different materials to generate charges. Their actual output is greatly affected by the paired triboelectric materials and surface contact. Therefore, this section first discusses the materials development and manufacturing, which is also the basis of research on W-TENGs. Current research begins with materials suitable for TENGs and progresses by processing them to enhance their electrical output characteristics. It also integrates advancements in materials science to develop new materials as required. Based on the continuous deepening of material research, this section is divided into the following parts: materials selection, contact optimization, chemical treatment, and the preparation of new materials.

3.1. Materials selection

TENGs offer the benefits of a wide range of materials choices and low production costs as the triboelectric effect can be induced in most materials. However, the output varies significantly with different material pairings, and the output of the same material in various environments may also differ. Therefore, the selection of materials plays a vital role in the output of W-TENGs. This section concisely reviews recent advancements in selecting the materials for W-TENGs.

In 2013, the first W-TENG designed by Yang *et al* [32] adopted a spherical structure, which became the typical

structure of W-TENGs. The W-TENG was fabricated by using the PTFE-PA films. Subsequent research has expanded the range of materials suitable for W-TENG manufacturing. As shown in figure 3(a), Wang *et al* [36] designed a new fully enclosed spherical W-TENG in 2015. They selected a polyhexamethylene adipamide (Nylon 6/6) ball, a polyimide (Kapton) film as the triboelectric layer materials, and aluminum (Al) foil as the electrode. They also made a preliminary comparison of the output performance of different paired triboelectric materials. The experiment was carried out by changing the moving sphere to a PTFE ball. It was found through experimental testing that the output power density of the Nylon/Kapton device is superior to that of the PTFE/Al device. In the W-TENG system developed by Demircioglu *et al* [84] in figure 3(b), polyurethane (PU) foam and poly(dimethyl siloxane) (PDMS) served as the paired triboelectric materials. This configuration not only enhanced the output but also significantly improved stability. No performance loss was observed even after 1200 cycles of stability measurement. Additionally, experiments were also conducted to evaluate the system's output in a simulated oceanic environment by testing it in a pool of water. Xia *et al* [85] changed the material of the moving sphere and used a natural wool ball, as shown in figure 3(c). Wool balls have excellent positive triboelectricity and fine wave-following properties in the ocean environment due to their lightweight. In the above works, the metallic material Al was used as the electrode. It is worth noting that metallic materials can also be used directly as dielectric materials. As shown in figure 3(d), the rolling spherical W-TENG (RS-TENG) designed by Wang *et al* [34] used silicone rubber balls. They studied the difference in output performance when copper (Cu) and Al were used directly as dielectric materials and found that the output of the Cu-silicone rubber had better performance than that of the Al-silicone rubber. The performances of other metal materials have also been widely studied. As shown in figure 3(e), Wu *et al* [33] designed the electrode stator consisting of eight sector-shaped grids made of conductive silver fabric.

The spherical structure is mainly designed for rolling mode, necessitating triboelectric materials that enable effective contact without impeding movement. Therefore, this requirement limits the selection of materials, and the selections for contact–separation mode are even more diverse. Wang *et al* [86] drew inspiration from the seaweed structures and fabricated a flexible seaweed-like W-TENG, namely the S-TENG shown in figure 3(f). The conductive ink was coated on the back of fluorinated ethylene propylene (FEP) and polyethylene terephthalate (PET) films, respectively. The ink formed a triboelectric pairing with FEP. Finally, the device was encapsulated with the PTFE tape, ensuring its waterproof capability. This design innovatively introduced the conductive ink material, which served as a triboelectric material and was directly used as an electrode. In figure 3(g), Saqib *et al* [87] directly used natural seagrass as a triboelectric positive material and developed a spray coatable W-TENG. The W-TENG coated with phyllospadix japonicus seagrass had good output performance and high stability. Moreover, seagrass was abundant and easy to obtain, which could greatly reduce production costs.

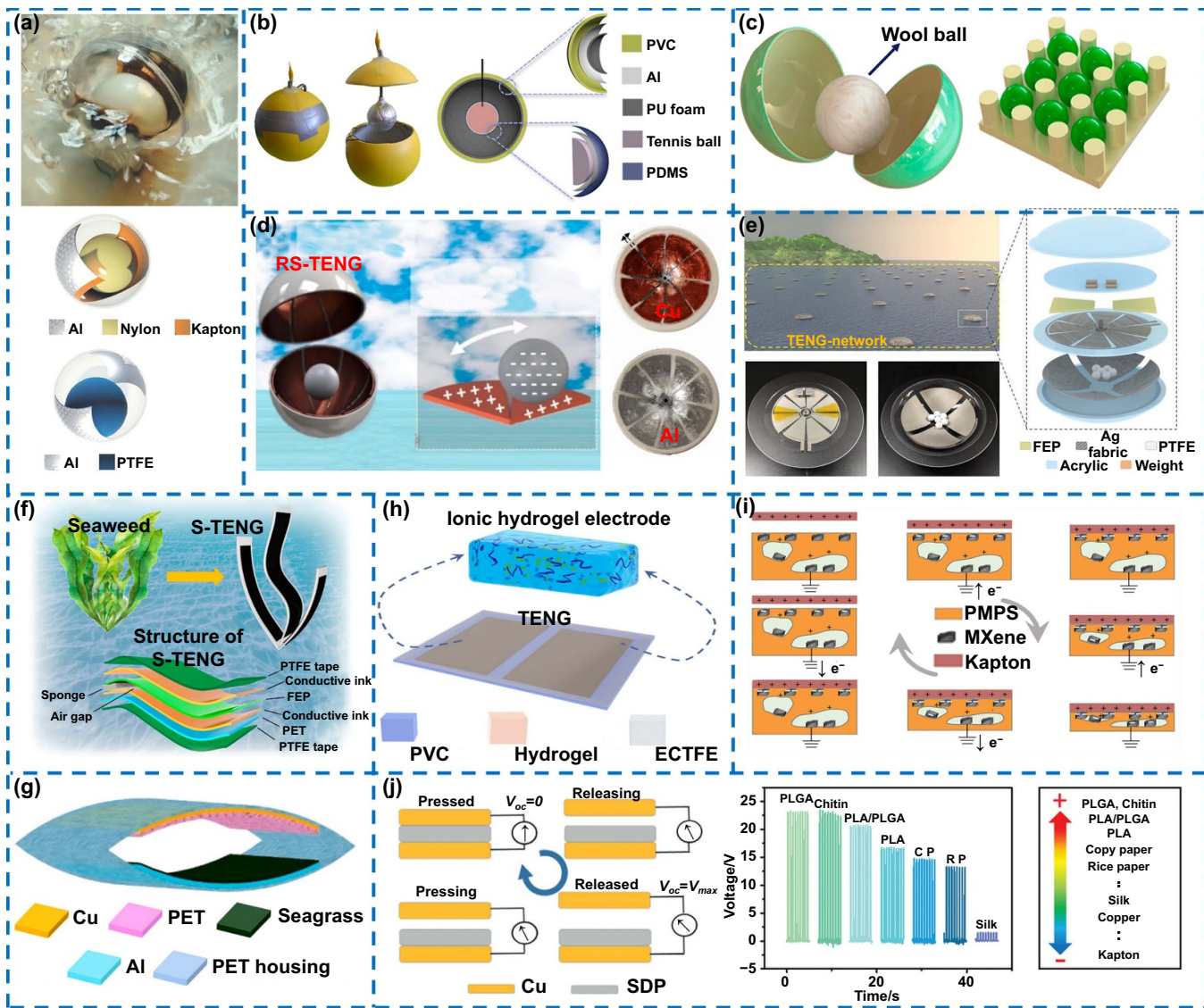


Figure 3. The materials manufacturing of W-TENGs. (a) Photograph of the fully enclosed spherical W-TENG and paired triboelectric materials. [36] John Wiley & Sons. © 2015 WILEY-VCH Verlag GmbH & Co. KGaA, Weinheim. (b) The W-TENG uses PU foam and PDMS served as paired triboelectric materials. Reprinted from [84], © 2022 Elsevier Ltd All rights reserved. (c) The W-TENG using wool balls. Reprinted from [85], © 2023 Published by Elsevier Ltd. (d) The RS-TENG. Reproduced from [34]. CC BY 4.0. (e) The use of conductive silver fabric in W-TENG. [33] John Wiley & Sons. © 2023 Wiley-VCH GmbH. (f) The flexible seaweed-like W-TENG. Reprinted (adapted) with permission from [86]. Copyright (2021) American Chemical Society. (g) The use of natural seagrass as triboelectric positive material in W-TENG. Reprinted from [87], © 2021 Elsevier Ltd All rights reserved. (h) The use of ionic hydrogel in W-TENG. Reprinted from [88], © 2022 Elsevier Ltd All rights reserved. (i) The working process of the W-TENG based on MXene. [89] John Wiley & Sons. © 2023 Wiley-VCH GmbH. (j) The working mechanism of a contact–separation W-TENG to evaluate triboelectrification properties. [55] John Wiley & Sons. © 2020 WILEY-VCH Verlag GmbH & Co. KGaA, Weinheim.

More importantly, it maintained the flexibility of the entire device.

Some popular materials have also been selected to make W-TENGs. The term ‘hydrogel’ first appeared in the literature in 1894 [90]. Hydrogels are generally a network of hydrophilic polymer chains, sometimes called colloidal gels [91]. Wang *et al* [88] used an ethylene chlorotrifluoroethylene (ECTFE) film and an ionic hydrogel electrode to construct a W-TENG, as shown in figure 3(h). The ECTFE had excellent electronegativity and a large number of fluorine groups, and the hydrogel had good conductivity even at low temperatures, making

it very suitable for the marine environment. The MXene, first reported in 2012, is a new large family of two-dimensional early transition metal carbides and carbonitrides [92]. Xu *et al* [89] found that MXene becomes negatively charged upon contact with PDMS and PTFE, while PDMS becomes positively charged when it comes into contact with Kapton. After adhering MXene into PDMS to form the PDA-MXene modified PDMS sponge (PMPS), Kapton came into contact with the PMPS, and electron transfer no longer only occurred between PDMS and MXene. Specifically, since the ability of Kapton to acquire electrons was weaker than that of PDMS, electrons

were transferred from Kapton to PDMS and then to MXene, thus improving the output. As shown in figure 3(i), all electrons were transferred to MXene, and this working process could be considered as a parallel connection of two TENGs.

As materials selection expanded, researchers embarked on a systematic comparison of the output characteristics of various materials. Chen *et al* [55] investigated the triboelectric properties of polylactic acid (PLA), poly (lactic-co-glycolic acid) (PLGA), PLA/PLGA, and several natural biodegradable materials. As shown in figure 3(j), the above materials were made into films of uniform size and thickness, and their output was evaluated in contact–separation mode. Based on these studies, they established a brief triboelectric series table to facilitate future materials selection. This also showed that the early triboelectric series table was insufficient for current use [93]. In recent years, many studies have been conducted to summarize new triboelectric series [94–96], but there was a lack of tools that could quantitatively characterize triboelectric electrification. Therefore, Zou *et al* [97] developed a standard measurement method to quantify the triboelectric characteristics of materials. This method has been applied to measure a wide range of commonly used materials in detail. Research in this area was attracting significant attention among the TENGs community, providing solid theoretical support for the selection of materials for TENGs [98].

3.2. Contact optimization

Materials selection serves as the foundation for TENGs, and surface contact is also crucial for electrical energy generation. According to its power generation principle, enhancing the contact area and optimizing the TE can significantly improve the output performance of TENGs. Therefore, numerous studies have been conducted to optimize the contact surface after selecting appropriate materials. This section primarily explores strategies for enlarging the effective friction area at the physical level, including surface roughening and the creation of micro- and nano-structures. It also examines how these approaches influence charge generation and thereby enhance output performance.

The generation of electrical output via triboelectric materials necessitates their continual contact and separation. Building on the discussion from the previous section, we suggest that moving spheres of various materials can be directly used as triboelectric materials. This is because the spherical structure can move with less external disturbance. However, a notable limitation of the spherical structure is its relatively small effective contact area when interacting with other triboelectric materials. Attention has been paid mainly to increasing the contact area while preserving the motion characteristics of these structures. As shown in figure 4(a), Yuan *et al* [99] expanded the frequency of point contacts by increasing the number of balls, thereby improving the effective contact efficiency. However, too many small balls could hinder independent movement. They concluded that a 60% coverage of the total area is the optimal value. Ouyang *et al* [100] posited

that an excessively large diameter of the balls could compromise the contact efficiency. So, they directly adopted a Cu particle design. As illustrated in figure 4(b), the Cu particles in the PTFE tube exhibited near-fluidic movement characteristics, significantly enhancing the contact area. Liquids, lacking a defined shape and conforming to the shape of their containers, offer unique opportunities for optimizing contact in TENGs. Cheng *et al* [101] developed a flexible core by filling silicone rubber with liquid, allowing the output to be modulated based on the thickness of the silicone shell. In a similar vein, Xia *et al* [102] introduced a balloon filled with sodium chloride/water solution into a square box. Inside the box, the tension of the balloon makes it self-supporting. When the box was excited by a wave even with a small amplitude, the balloon could effectively contact the wall of the box to generate electricity (figure 4(c)). The studies mentioned above [101, 102] used soft contact to enhance output performance, and their mechanisms have been studied in depth. Luo *et al* [103] discovered that while hard contact between a moving sphere and its casing produced a high impact force, it led to minimal surface strain, resulting in suboptimal output. In contrast, soft contacts allowed for a larger contact area and more rapid charge accumulation, but they exhibited insufficient impact strength. To overcome this limitation, they adopted an innovative approach by incorporating a layer of cellulose nanocrystals and Ecoflex on the silicone substrate of the sphere’s surface. The designed ‘Lucky Bag’ core is shown in figure 4(d). They also showed the schematic diagram of the corresponding electron potential well model. In addition to optimizing the moving sphere, the triboelectric materials could also be processed. Chen *et al* [104] fabricated nano-micro structures on the PTFE surface in contact with the spheres, as shown in figure 4(e). Chau *et al* [105] fabricated polyvinyl chloride (PVC) with a honeycomb structure surface, which significantly increased the effective contact area, as shown in figure 4(f).

Not only W-TENGs with spherical motion contact need surface contact optimization, but other modes can also benefit from the above method. Figure 4(g) shows that Lin *et al* [106] set up a moving part with a spring and placed flexible dielectric fluff on the front end. Soft contact for pendulum motion was achieved by creating nanowire structures on the PTFE surface. Testing three different devices confirmed that the spring and fluff structure design could help increase the effective contact area and improve the output. Furthermore, some simple physical etching methods were also used to optimize the contact surface design. Chen *et al* [39] used reactive ion etching to form nanowire arrays on the surface of PTFE, and also created nanopores on the Al electrode in contact with it (figure 4(h)). Lin *et al* [109] utilized inductively coupled plasma etching to develop microstructures on the PTFE surface. Li *et al* [110] used surface plasma treatment to establish uniform nanowires on the PTFE surface and also created nanopores on the Al electrode.

As discussed above, the flow characteristics of liquids facilitate the formation of soft contacts, thereby increasing the contact area, and liquid–solid mode TENGs can be directly produced using these properties. The liquid–solid W-TENG

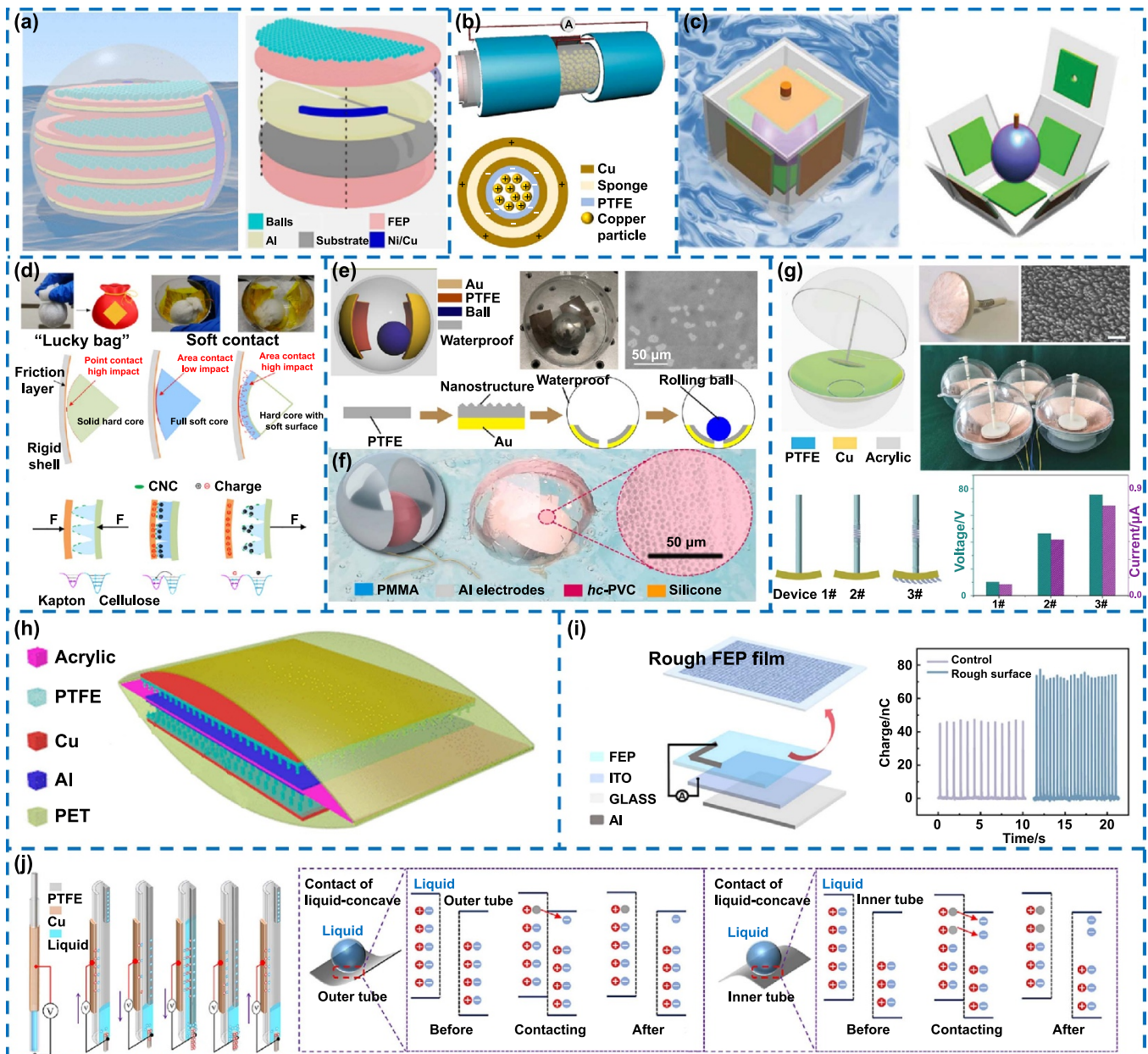


Figure 4. The contact optimization of W-TENGs. (a) The enlarged view of the W-TENG unit with a large number of balls. Reprinted (adapted) with permission from [99]. Copyright (2021) American Chemical Society. (b) The W-TENG with Cu particles. Reprinted from [100], © 2022 Elsevier Ltd All rights reserved. (c) Structure expansion diagram of the W-TENG using a water balloon. [102] John Wiley & Sons. © 2020 WILEY-VCH Verlag GmbH & Co. KGaA, Weinheim. (d) The photograph and surface contact diagram of the 'Lucky Bag'. Reproduced from [103]. CC BY 4.0. (e) The device structure and the schematic fabrication process on the PTFE surface. Reproduced from [104]. CC BY 4.0. (f) The microstructure of hc-PVC electret. Reproduced from [105]. CC BY 4.0. (g) Schematic illustration and output performance of the W-TENG composed of a cambered triboelectric layer and pendulum-like component. [106] John Wiley & Sons. © 2021 Wiley-VCH GmbH. (h) The nanowire arrays on the surface of PTFE in W-TENG. Reprinted (adapted) with permission from [39]. Copyright (2015) American Chemical Society. (i) The creation of surface roughness of solid friction layer. Reprinted (adapted) with permission from [107]. Copyright (2024) American Chemical Society. (j) The schematic diagram of the curvature effect on the liquid–solid interface with different curvatures. Reprinted from [108], © 2023 Elsevier B.V. All rights reserved.

reported by Zhou *et al* [107] also used surface roughening techniques on an FEP film (figure 4(i)). Specifically, they polished the FEP surface using sandpaper of a specific grit and subsequently cleaned it with absolute ethanol, thus increasing the surface area without causing damage. Under identical experimental conditions, the surface-treated device demonstrated a 58.70% increase in charge transfer, rising

from 46 nC to 73 nC compared to the untreated counterpart. Wang *et al* [108] investigated the influence of surface curvature on the electrical energy generation of liquid–solid W-TENG. They generated electrical energy through periodic contact–separation of PTFE rods and deionized water, as shown in figure 4(j). Materials with high curvature surfaces tend to have lower surface energy and result in more negative

charges. Recent developments have seen W-TENGs employing a variety of liquids, including deionized water [111], distilled water [112], seawater [113], and mercury [114], all of which have demonstrated remarkable output performance. This also proved that W-TENGs have robust adaptability when facing complex marine environments.

3.3. Chemical treatment

In the preceding section, we extensively discussed the utilization of physical methods for contact optimization to enhance output, highlighting their operational simplicity and cost-effectiveness. However, further consideration is needed in terms of wear resistance, and there is a limited selection of triboelectric materials. To address these challenges, researchers have innovated numerous chemical treatment techniques, including particle/ion injection, surface chemical modification, and functional group manipulation, among others [35]. This subsection introduces how to choose suitable chemical treatments according to the specific materials and application environments, aiming at augmenting both the materials' reliability and device output performance.

A key step in TENGs is the electrostatic induction due to surface charges, so unipolar charged particles/ions can be injected into materials to enhance electrostatic induction. Zhang *et al* [115] placed multiple layers of wavy-structured robust W-TENGs (WS-TENG) on each side of a regular dodecahedron (figure 5(a)). The basic process of injecting electrons into the FEP film that makes up the WS-TENG is also shown. The cathode of the power supply was connected to the needle, while the anode and ground were linked to the Cu electrode deposited on the back of the FEP. They pointed the needle tip toward the FEP surface at a vertical distance of 10 cm and applied a polarization voltage of 5 kV for 5 min. In addition to injecting electrons into the FEP film, other electronegative materials could also use this method. As shown in figure 5(b), Xu *et al* [116] used the same method to inject electrons into a PTFE film to enhance charge. Tao *et al* [117] used corona discharging, a more economical and simple method, to pre-inject ionized charges into the FEP film as a constant bias. The specific process is shown in figure 5(c), where the FEP film was installed on both sides of the substrate and then charged by the corona discharging systems based on a triode-needle-grid setup. The ionized and partially conductive air around the tip was driven to the lower potential grid, and charged particles were uniformly injected into the electret through the electrostatic field between the grid and the substrate. The substrate was heated for multiple cycles to avoid being neutralized by air. After cyclic discharging on both sides of the FEP film, it had excellent stability and could be folded to form a three-dimensional (3D) W-TENG. Tripathy *et al* [118] developed the floating W-TENGs using FEP films and chemically modified nylon films, as shown in figure 5(d). The atomic force microscopy (AFM) images of the original and modified nylon film in 60% formic acid solution are shown, respectively. The chemical etching process significantly increased the roughness of the nylon film from 72 pm to 328 pm, potentially improving its triboelectric performance.

About the functional group manipulation, Ding *et al* [119] achieved the ability to control the gain or loss of charge by modifying the functional groups on the surface of cellulose. They prepared a hyperbranched polymer with abundant electron-releasing amino groups, and polyethyleneimine (PEI) was incorporated to improve the triboelectric polarity further (forming a system that is therein referred to as PEI-S-CNF-W-CMF). They used PEI-S-CNF-W-CMF as a positive triboelectric material through physical doping and chemical modification, as shown in figure 5(e). The PEI-S-CNF-W-CMF specifically involved spraying silanized cellulose nanofibers (S-CNF) onto the surface of the paper, which exhibited different degrees of wrinkling. The histogram showed a significant increase in surface potential from 189 mV to 388 mV, which correlated with an increase in the number of $-\text{NH}_x$ groups. This illustrated a direct relationship between the number of amino groups and the enhancement of surface potential. Zhang *et al* [120] released electron functional groups through methyl to improve the CNF triboelectricity and electrical output performance of the CNF-based TENG. They prepared a methylated superhydrophobic CNF film as the positive triboelectric layer, and the preparation process is shown in figure 5(f). The film's roughness also improved through modification, with the root mean square surface roughness being increased from 56.68 nm to 72.61 nm. At the same time, the water contact angle reached 154.7°.

3.4. New materials preparation

W-TENGs primarily consist of triboelectric material pairings and conductive electrodes. In section 3.1, we discussed the selection of high-performance triboelectric and electrode materials that are easy to manufacture. However, most of them are non-renewable, non-biodegradable polymer and hard metal materials, limiting their economic viability and practical application [121–123]. As materials science research progresses, the large-scale production of materials tailored to specific needs has become feasible. Therefore, researchers have recently been exploring the preparation of new materials for manufacturing W-TENGs, paying particular attention to degradable, renewable and other environmentally friendly triboelectric materials.

Pang *et al* [124] prepared an alginate film that could be degraded in the ocean, and its preparation process is shown in figure 6(a). Sodium alginate, extracted from ocean plants, was placed in deionized water and stirred until completely dissolved. The solution was then pre-frozen at -5°C to remove entrained air and freeze-dried at -55°C . To improve strength and flexibility, it was cross-linked with 5% (w/w) calcium chloride solution for 10 min and then left to dry naturally. From the comparison of chemical structural formulas before and after preparation, it could be seen that calcium and sodium ions were exchanged. The chelate could exchange with the oxygen atoms, allowing the alginate chains to combine firmly, enhancing the synergistic effect. The W-TENG, made of calcium alginate film, green biodegradable material

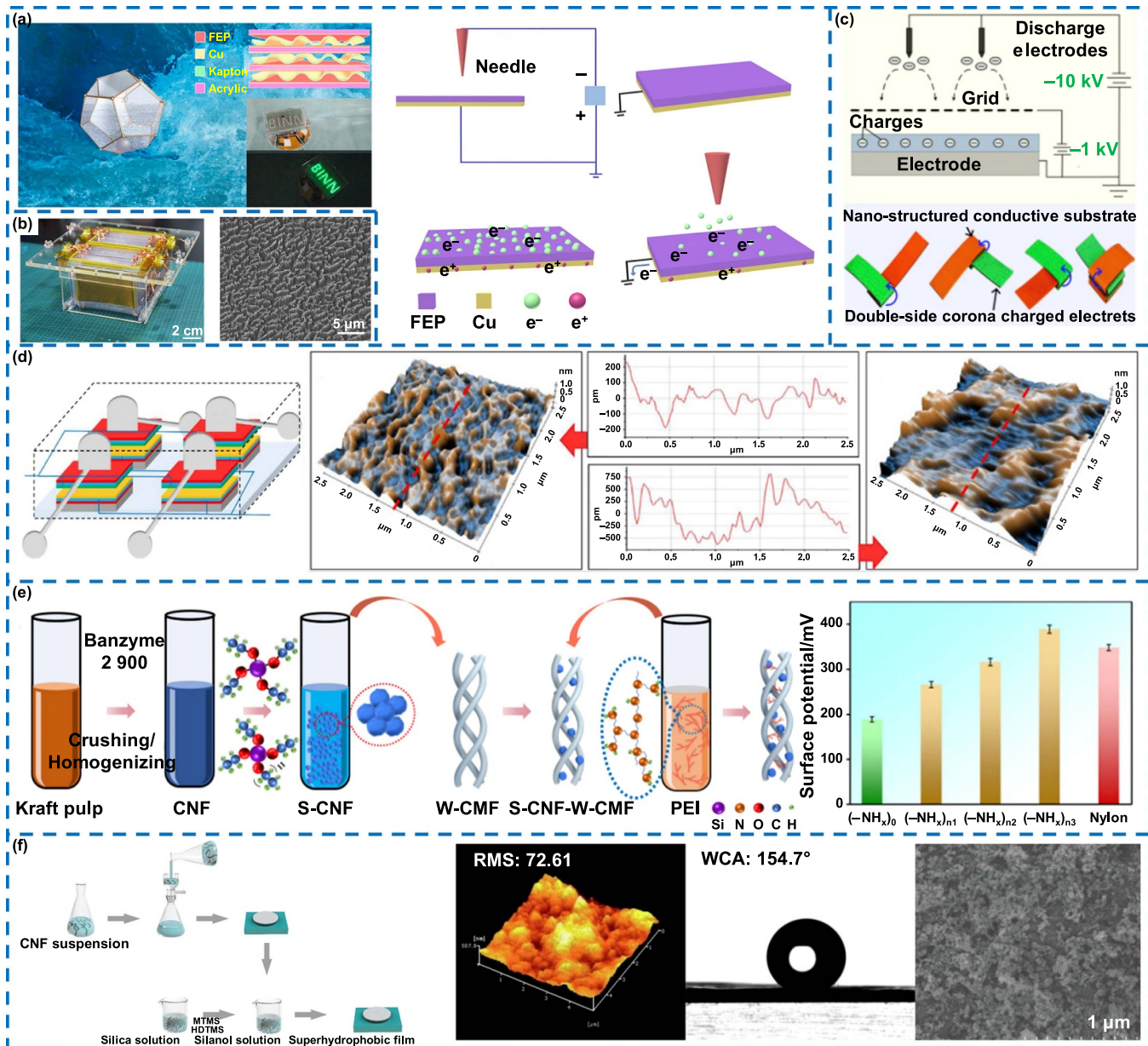


Figure 5. The chemical treatment of W-TENGs. (a) The schematic diagram of WS-TENG and basic process on the FEP film. Reprinted from [115], Copyright © 2016 Elsevier Ltd All rights reserved. (b) The structure of W-TENG and nanostructures on the PTFE surface. Reprinted from [116], © 2016 Elsevier Ltd All rights reserved. (c) Constructing 3D origami W-TENG folded using two polymer strips. Reprinted from [117], © 2019 Elsevier Ltd All rights reserved. (d) The interior schematic design of the W-TENG and the AFM images. Reprinted from [118], © 2023 The Authors. Published by Elsevier B.V. on behalf of Shandong University. (e) The schematics of the preparation process of the micro/nanostructure of PEI-S-CNF-W-CMF and the surface potential of different number densities of $-\text{NH}_x$. Reprinted from [119], © 2022 Published by Elsevier B.V. (f) The preparation process and modification mechanism of the CNF film and its characteristics. Reprinted from [120], © 2022 Elsevier B.V. All rights reserved.

PLA, and a small amount of metal materials that could corrode in the ocean, was degradable and friendly to the marine environment. The most critical issues faced in collecting ocean energy are hydrophobicity and anti-corrosion. In response to the hydrophobic requirements of surface materials of marine structures, Wang *et al* [125] prepared fluorine-modified acrylate resin materials as coatings. The preparation process was simple, as shown in figure 6(b). The material not only showed good hydrophobicity but also increased the charge transfer rate between triboelectric materials due to the strong

electron affinity of fluorine atoms. By studying the composition of the coating, the triboelectric output performance was optimized, and an organic coating TENG was designed, which could closely combine the performance of the coating itself with the power generation function. Zaw *et al* [126] fabricated a mat-shaped solid-liquid W-TENG (MSLT), and its manufacturing process is shown in figure 6(c). The new material used was a conductive polymer formed by mixing 15 wt% carbon black and PDMS, which gave MSLT excellent flexibility and hydrophobic properties. Moreover, MSLT was also

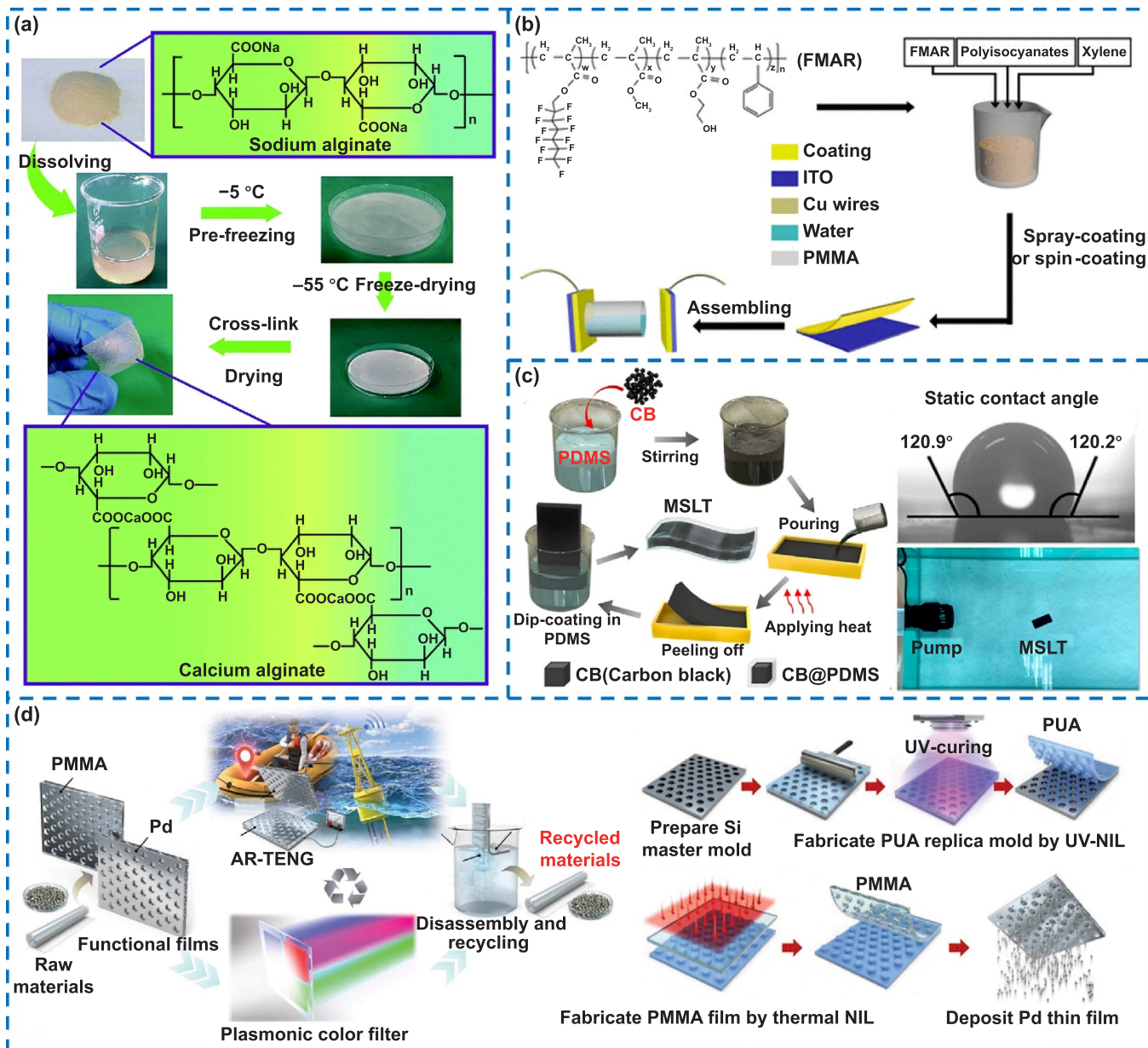


Figure 6. The new materials preparation. (a) The fabrication process for the calcium alginate film and the chemical structural formula in the insets. Adapted from [124] with permission from the Royal Society of Chemistry. (b) The preparation process of the fluorine-modified acrylate. Reprinted (adapted) with permission from [125]. Copyright (2020) American Chemical Society. (c) Schematic diagram of the structure and fabrication process of the MSLT. Reprinted from [126], © 2022 Elsevier Ltd All rights reserved. (d) The recycling process and the functional film fabrication. [127] John Wiley & Sons. © 2022 Wiley-VCH GmbH.

corrosion-resistant and could be placed directly in the waves to generate electricity. In response to the demand for eco-friendly W-TENGs, Ahn *et al* [127] involved an all-recyclable W-TENG (AR-TENG) with stable mechanical and chemical properties. Its overall manufacturing, application, and recycling processes were as follows, as shown in figure 6(d). The UV-based nanoimprint lithography (UV-NIL), thermal NIL and e-beam evaporation technologies were used to prepare the new material. Specifically, a nanopatterned PU acrylate mold was made on a silicon master mold through UV-NIL, and then the PMMA film was pressed using thermal NIL. Finally, the palladium (Pd) film was deposited by an e-beam evaporator.

When an AR-TENG was damaged or expired, it could be remanufactured without requiring additional materials or generating waste.

4. Structural design and fabrication

Through the summary of the previous section, we have offered a comprehensive overview of the materials appropriate for W-TENGs, detailing their properties and optimization techniques. Structural design is the pillar of W-TENG research. Only a robust and dependable structure can fully utilize the

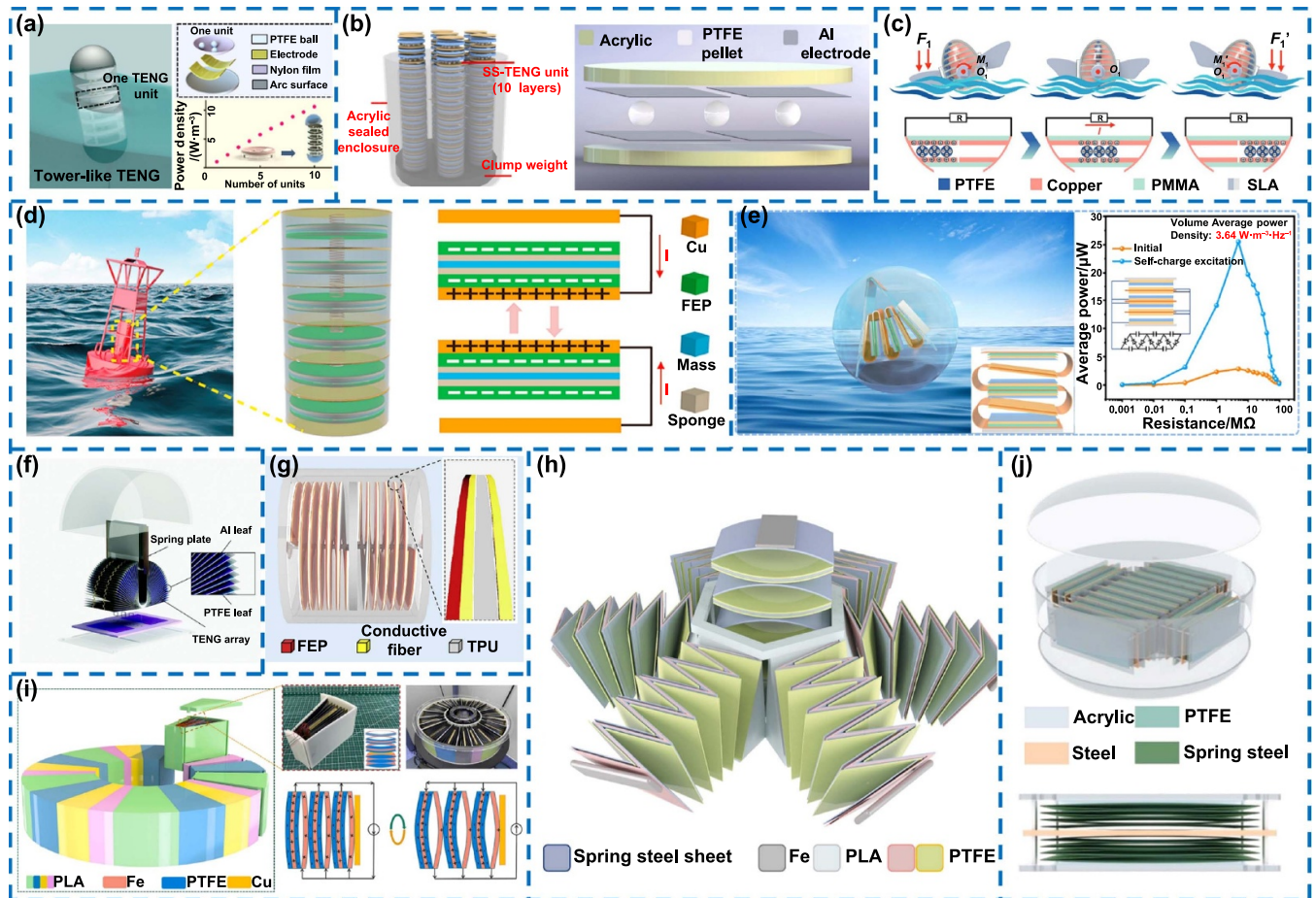


Figure 7. The multi-layer structure W-TENGs. (a) The multi-layer tower-like W-TENG. Reprinted (adapted) with permission from [58]. Copyright (2019) American Chemical Society. (b) The multi-layered sandwich W-TENG. Reprinted from [62], © 2021 Elsevier Ltd All rights reserved. (c) The FETENG with a bionic fish structure. Adapted from [131], with permission from Springer Nature. (d) The multi-layer W-TENG with six basic units. Reprinted from [132], © 2019 Elsevier Ltd All rights reserved. (e) The swing mode multi-layered self-charge excitation W-TENG. Reprinted from [133], © 2023 Elsevier Ltd All rights reserved. (f) The open-book-like W-TENG. Adapted from [134] with permission from the Royal Society of Chemistry. (g) The anaconda-shaped spiral multi-layered W-TENG. Reprinted from [135], © 2022 Elsevier Inc. (h) The flower-like W-TENG. Reprinted from [136], © 2021 Elsevier Ltd All rights reserved. (i) The O-ring-like W-TENG. Reprinted from [137], © 2022 Elsevier Ltd All rights reserved. (j) The multi-arch structure W-TENG. Reproduced from [138]. CC BY 4.0.

properties of materials and ensure consistent output. With the development of materials research and the needs of different scenarios, various W-TENGs with different structures have been manufactured [76, 128, 129]. The rapid development of 3D printing technology provides great potential for manufacturing TENG prototypes and their components (including triboelectric layers, electrodes, device frames, and additional components.) with unique structures [130]. According to the different array modes of power generation units inside W-TENGs and their related kinetic energy transfer forms, this section classifies and introduces some typical structures. It mainly includes multi-layer, channel, elastic, and rotating structures.

4.1. Multi-layer structure

Early research mainly used the structure of a single sphere with a single motor ball placed inside. This structure is simple to

manufacture and easy to move, but it wastes internal movement space and occupies a large ocean area. In subsequent studies, researchers begin to pay attention to how to improve the space utilization of the structure. By stacking multiple triboelectric layers in the vertical or horizontal direction, the output of W-TENGs per unit ocean area can be improved nearly linearly. Moreover, the power generation unit is unified, enabling fast and large-scale manufacturing. Xu *et al* [58] innovatively proposed a multi-layer tower-like W-TENG that could collect wave energy in any direction (figure 7(a)). Each layer was structured as a unit, with multiple PTFE balls placed inside to roll on a nylon film, and electrodes were attached to the back of the films to collect alternating current (AC). They found that the power density increased linearly from $1.03 \text{ W} \cdot \text{m}^{-3}$ to $10.6 \text{ W} \cdot \text{m}^{-3}$ when the number of units connected in parallel increased from 1 to 10. In figure 7(b), Wang *et al* [62] designed a multi-layered sandwich W-TENG. The gap between the layers was slightly larger than the diameter of

the PTFE ball, allowing it to contact the upper and lower electrodes at the same time. By integrating seven such W-TENGs into a buoy, they succeeded in lighting up 12 W high-intensity LEDs for navigational purposes. Jing *et al* [131] created a 3D fully enclosed W-TENG (FETENG) with a bionic fish structure, using parallel stacked multi-layer substrates filled with diminutive balls to optimize internal space utilization. Its motion state and power generation principle are shown in figure 7(c). Under the excitations of water waves, the bionic fin generated a vertical downward force, driving the entire device and causing the internal balls to slide and generate electrical output. In the above studies, through the high-precision processing of 3D printing technology, the gaps between layers could be accurately controlled.

W-TENGs based on contact–separation mode are more convenient when manufacturing multi-layer structures. Xi *et al* [132] designed a multi-layer W-TENG with six basic units, as shown in figure 7(d). Driven by waves and springs, the mass block cyclically vibrated up and down, causing the FEP films on both sides to continuously contact and separate from the Cu films to produce AC output. Li *et al* [133] fabricated a swing mode multi-layered self-charge excitation W-TENG (MSCE-TENG) to increase the contact area and charge accumulation rate to improve the output. Figure 7(e) shows that the acrylic plates were arranged up and down as the base, and foam was added to the Kapton base material as a buffer layer. Wave-driven pressure on the substrate enabled multi-layer contact–separation of the PVDF layers and the Cu films. Under the wave excitation, MSCE-TENG obtained an average power of $3.64 \text{ W} \cdot \text{m}^{-3} \cdot \text{Hz}^{-1}$ (corresponding output power: $25.5 \mu\text{W}$), which was nine times that of other common multi-layer structures. The open-book-like W-TENG prepared by Zhong *et al* [134] had more layers (figure 7(f)), the bottom end was fixed, and each page (layer) could be accompanied by a swinging motion of the upper part. Yuan *et al* [135] designed an anaconda-shaped spiral multi-layered W-TENG, as shown in figure 7(g), which achieved a space utilization rate of 93.75%. Due to electrostatic adsorption, the spiral multi-layer structure could avoid incomplete separation of the dielectric layers and the electrodes.

Planar contact–separation can effectively respond to motion perpendicular to the contact surface, but how to collect energy in other directions becomes a key issue. Wen *et al* [136] designed a flower-like W-TENG for six degrees of freedom kinetic energy collection. The petals in six directions were six power generation units, as shown in figure 7(h). Under the action of waves, each generating unit continuously ‘flowered’ (separated) and ‘folded’ (contacted) to generate electrical energy. This structure was suitable for various motions, including horizontal and vertical translation, rotational motion and swing. Li *et al* [137] prepared an O-ring-like W-TENG (O-TENG) by adjusting the flexible splicing of sector-shaped TENG blocks at different angles. The single sector-shaped block and the assembled O-TENG are shown in figure 7(i). This structure achieved omnidirectional wave energy collection. The O-shaped design of the multi-sector block made the frequency response fully adjustable, while

its dispersed mass and non-linear surface made it easier to respond to water waves. Another problem with multi-layer planar structures is that they are not easy to move under low-frequency and low-amplitude waves due to their lightweight. To address this, Feng *et al* [138] used a multi-arch structure to ensure sufficient contact and also placed a steel plate in the center of each TENG block (figure 7(j)). The weight of the steel plate allowed the W-TENG to generate electricity normally, even at an angle of 7° . The entire device consisted of a central cylinder with oblate spherical shells at the top and bottom, giving it a flat structure that could easily respond to waves and did not affect the output even if it overturned. Moreover, the diameter of the core cylinder of the device reached 0.5 m, which provided a feasible strategy for the large-scale design of W-TENGs.

4.2. Channel structure

In the previous subsection, we mentioned that multiple balls can be placed on each layer to improve space utilization. However, this improvement has an upper limit. The disadvantage of the multi-layer structure is that its stability is poor when the number of layers is too large. In addition, if there are a large number of small balls inside the structure, their movements may interfere with each other. In some movement directions, they may not effectively contact the electrodes. Therefore, researchers have explored the implementation of channels to constrain the movement paths of these structures. These channels serve to direct the internal motion, ensuring optimal contact with the opposing dielectric material electrodes. Consequently, the channel structure has significant advantages with high volatility and changeable directions, especially in an ocean environment.

Yang *et al* [139] designed a self-assembly network, whose basic unit adopted a multi-layer multi-channel design and had a 3D electrode structure (figure 8(a)). Four longitudinal and thirteen transverse electrode plates were prepared on a printed circuit board with double-sided Cu patterns, which were welded together to create internal channels and form the 3D electrodes. The FEP particle balls were placed in the channel. The channels cleared the entire movement paths of the FEP particles and increased the number of fillings. The contact between the FEP particles, which occupied about half of the channel volume, and the Cu electrodes generated electrical energy. Liu *et al* [140] developed a nodding duck structure multi-channel W-TENG, whose structure is shown in figure 8(b). The shape was designed as a nodding duck block, which could rotate around its axis after being affected by waves. The entire structure was divided into three layers, with each sharing electrodes and dielectric films to efficiently utilize space. Each layer was equipped with channels, and the nylon balls rolled freely under the excitation of waves and the guidance of the channels. They also achieved the synchronous movement of the nylon balls by changing the number of channels and the connection methods among the channel units, ensuring stable and efficient output.

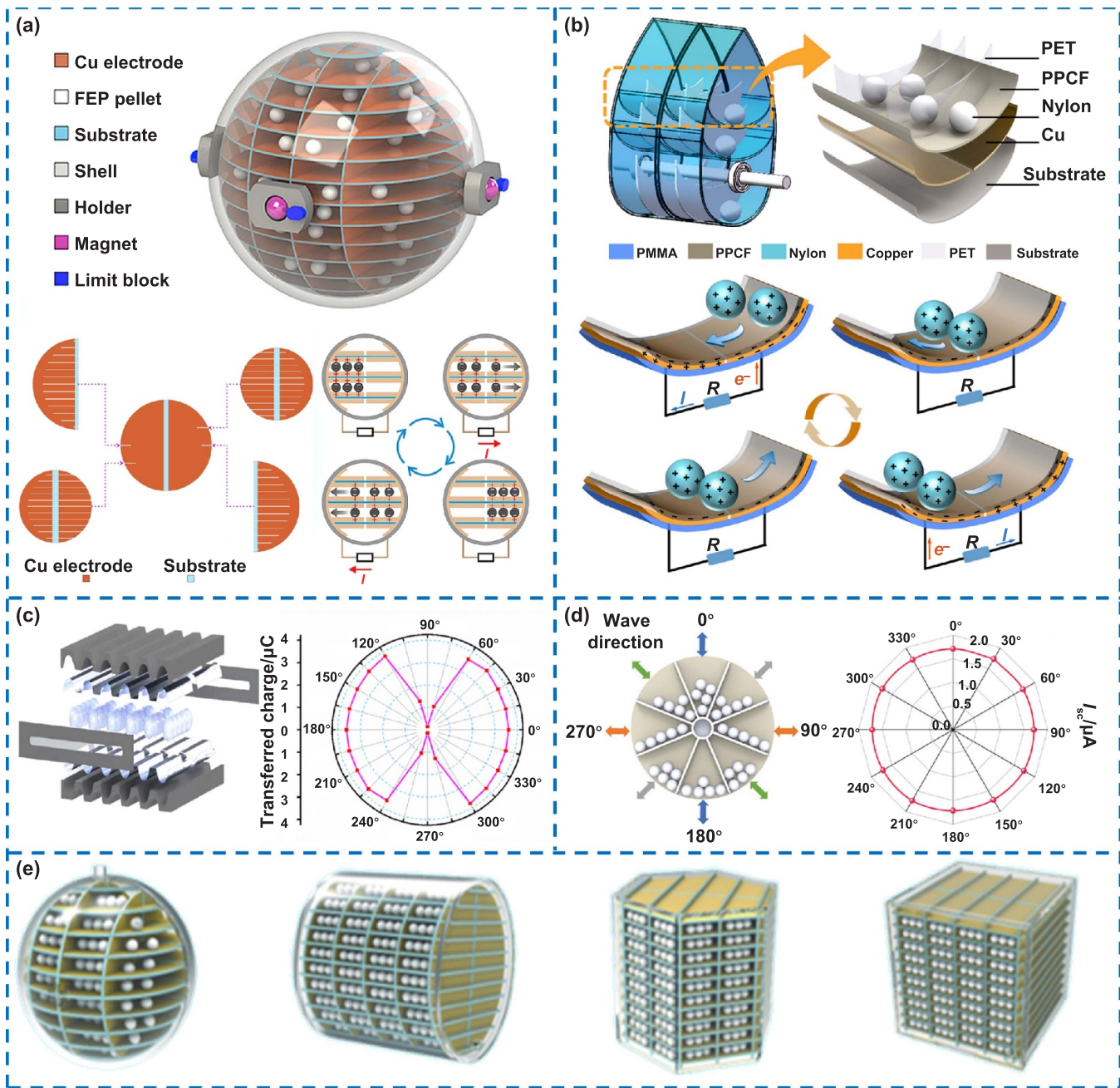


Figure 8. The channel structure W-TENGs. (a) The schematic structure of the W-TENG unit and the working principle. Reprinted from [139], © 2019 Elsevier Ltd All rights reserved. (b) The nodding duck structure multi-channel W-TENG. Reprinted (adapted) with permission from [140]. Copyright (2021) American Chemical Society. (c) The stackable W-TENG. Reproduced from [141]. CC BY 4.0. (d) The omnidirectional multi-channel spherical structure W-TENG. [142] John Wiley & Sons. © 2024 Wiley-VCH GmbH. (e) The schematic diagrams of the four structures. Adapted from [143], with permission from Springer Nature.

The existence of channels can guide the path of the moving structure, but the impact of the wave direction on the output when the path is determined must also be studied. Wang *et al* [141] designed a stackable W-TENG (S-TENG) featuring channels with a wavy cross-section to increase the contact area between the PTFE balls and the electrodes during rolling. This design allowed for rapid responsiveness to wave excitation, with the directional influence of wave excitation, as depicted in figure 8(c). Under most conditions, except when the wave direction aligns perpendicularly to the channels (at 90° and

270°), the charge transfer by the S-TENG was desirable, yielding effective output in most orientations. Because as long as there was a little component force along the channel, the balls could complete effective movement under the guidance of the channel, allowing the charges to be transferred entirely. The inherent disorder in wave movement makes the S-TENG particularly effective for wave energy harvesting, as it maintains a good output despite these conditions. Of course, omnidirectional wave energy collection can also be achieved through channel design. Ying *et al* [142] developed an omnidirectional

multi-channel spherical structure W-TENG (OMS-TENG). The OMS-TENG used three TENG layers, and each layer was divided into eight fan-type TENGs (FTENG) through channels. Due to the channel structure, the PTFE balls in each FTENG could roll freely without affecting each other. As shown in figure 8(d), the output performance of OMS-TENG remained stable under different wave directions from 0° to 360°. The channel structure ensured that after waves impacted the outer shell, the internal motion structure moved under the guidance of the channel. Duan *et al* [143] studied four common shell shapes: sphere, cylinder, regular hexagonal prism and cube, as shown in figure 8(e). They kept the diameter of the PTFE balls, the electrode spacing and the number of grids in different shapes the same. Four shapes of W-TENG were tested under the same simulated wave conditions, and the cubic structure was found to have the highest output performance, which provided necessary guidance for the overall shape design of the W-TENGs with channel structures.

There are still some flaws in the channel structure design that need to be addressed. First, the design of the internal structure has some constraints. For example, in order to move smoothly in the channel, only spherical or columnar moving parts can be generally used. Second, when the wave height is low, the moving structure may be unable to complete the entire journey and, therefore, cannot work effectively.

4.3. Elastic structure

Ocean waves often have large amplitudes and low frequencies, which means that many structures cannot operate effectively or even overturn directly. Researchers have adeptly addressed this issue through the incorporation of an elastic structure. Primarily, the elastic structure can serve as a buffer and then fully release the stored potential energy again. In addition, the elastic structure can also be used to adjust the device's response frequency. In most cases, low-frequency wave motion is converted into high-frequency elastic component oscillations to improve energy harvesting efficiency.

In figure 9(a), Xiao *et al* [144] fabricated a spring-assisted multilayer structure spherical W-TENG, which adopted a zig-zag structure with a mass block and rigid spring placed above it. Triggered by strong water waves, the spring's elastic force compresses the multi-layer TENG, enabling full contact and separation. In figure 9(b), Lei *et al* [145] designed a butterfly-inspired W-TENG (B-TENG), which could trigger two different modes of motion to obtain more wave energy. As long as there were wave excitations, the PTFE sheets on the flapping wings could flap up and down or swing left and right to come into contact with part of the Cu films. The spring's restoring force enables separation from one part of the Cu films and contact with another, while an additional mass block enhances the deformation effect. Liang *et al* [146] further prepared a spherical W-TENG composed of six multilayered TENGs symmetrically positioned in different directions. As shown in figure 9(c), the movements in the six directions did not affect each other, and energy conversion could always be achieved regardless of the triggering angle. Further, this team

[147] also coupled the spring and swing structures to optimize output performance by adjusting the spring length and counterweight mass, as shown in figure 9(d). They found that the presence of the spring not only increased the frequency of motion, but also enhanced the reciprocation of the swing component. Wang *et al* [148] reported a structure in which the inner and outer tetrahedrons could be contacted and separated face-to-face through springs and matched the first-order oscillation frequency of the structure with the major frequency of ocean waves. The structure is shown in figure 9(e). The vertices of the inner tetrahedron were connected to those of the outer tetrahedron by springs, allowing the inner structure to oscillate with wave motion. The spring tension was adjusted via the nut to allow parallel contact between the two tetrahedrons' surfaces.

Elastic structures can be achieved not only through springs but also by manufacturing structures with elastic functions. Liang *et al* [149] designed a W-TENG that could store elastic potential energy through a spring-like shape without additional springs, as shown in figure 9(f). Silicone was chosen as the substrate due to its flexibility and ease of fabrication. A flat spring-like shape was formed through 3D printing technology, and then Cu electrodes and PET films adhered to both sides of the 'spring'. Additionally, a Cu ball placed in the center could drive independent TENG units to work separately under the action of waves. Liu *et al* [150] used thermoplastic PU as the substrate and completely filled the spherical structure into a multilayered helical spring-like structure (figure 9(g)), with a space utilization rate of 92.5%. The device was divided into two mirror-symmetrical semispherical units, each with nine spring coils (number of layers) and a stiffness coefficient of 48 N·m⁻¹. When the spherical shell was triggered by water waves, the internal base material stretched and compressed left and right, causing the Cu electrode and FEP triboelectric layer to contact and separate. The mutual repulsion properties of magnets, similar to elasticity, are also exploited. As shown in figure 9(h), Jung *et al* [151] placed a magnet on the rotor and stator, respectively, so that the same poles faced each other. With the repulsive force of the magnet, the rotation angle of the rotor rotated by the wave action was increased. The advantage of the elastic structure is further reflected in its ability to collect fragmented and irregularly distributed wave energy, a result of mutual wave interference. Yang *et al* [152] proposed a swing self-regulated W-TENG (SSR-TENG) that could efficiently collect low-grade, high-entropy ocean-breaking wave energy using a spring structure. As shown in figure 9(i), SSR-TENG consisted of a float, a spring support and a TENG unit. The spring support could swing to collect wave energy in all directions. By increasing the swing angle and damping, it was self-adjusted to collect the mechanical energy of waves more effectively.

It needs to be noted that whether elastic structures are used to store energy or increase frequency, their performance has a threshold. Exceeding the threshold necessitates an assessment of potential large-scale impact damage to the structure when utilizing W-TENGs in a marine environment. Moreover, the existence of spring structures or spring-like structures increases the size of W-TENGs.

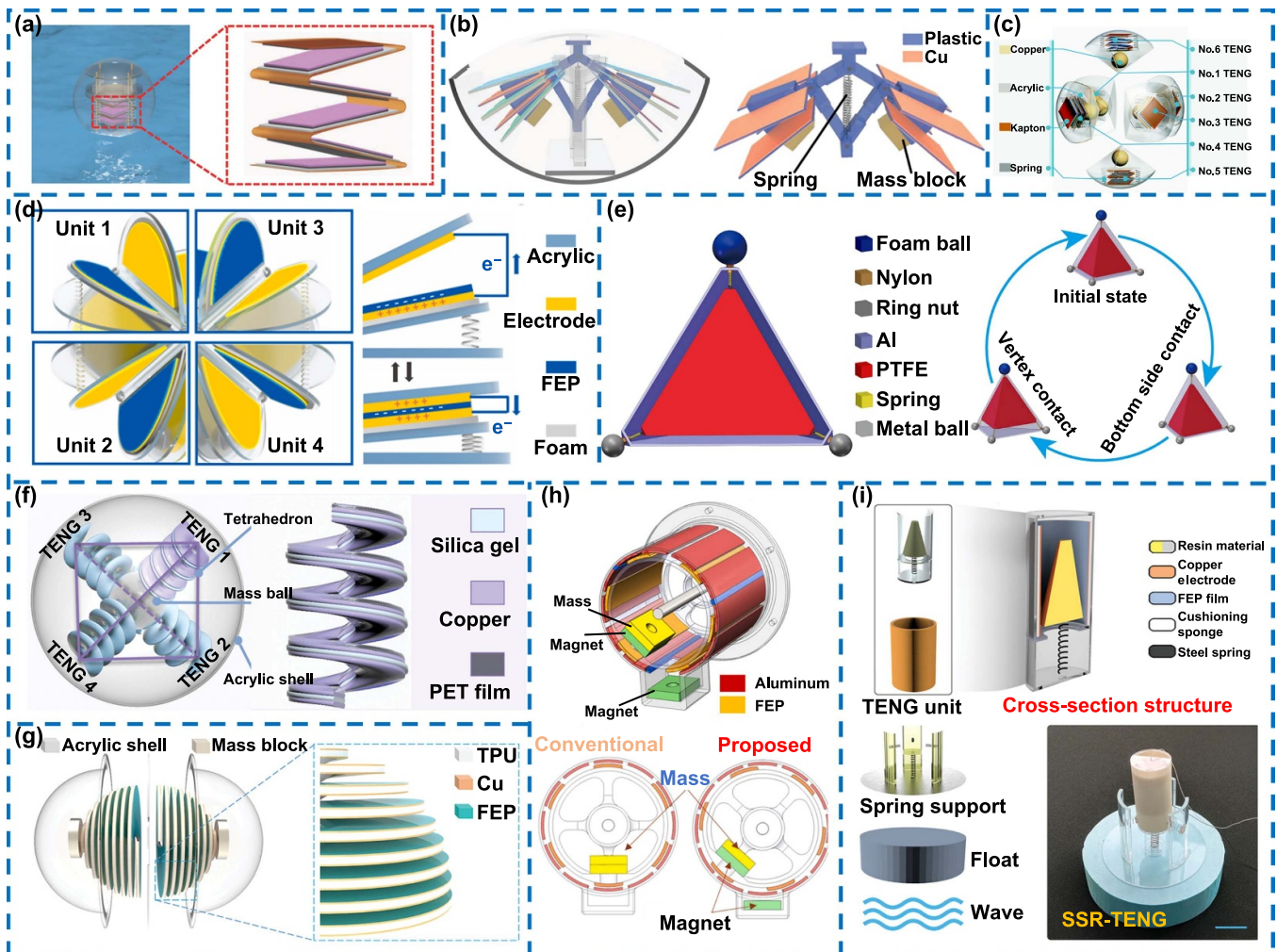


Figure 9. The elastic structure W-TENGs. (a) The spring-assisted multilayer structure spherical W-TENG. [144] John Wiley & Sons. © 2018 WILEY-VCH Verlag GmbH & Co. KGaA, Weinheim. (b) The butterfly-inspired W-TENG. [145] John Wiley & Sons. © 2018 WILEY-VCH Verlag GmbH & Co. KGaA, Weinheim. (c) The six multilayered TENGs. Adapted from [146] with permission from the Royal Society of Chemistry. (d) The relative positions of four basic units and their working principle in the spherical TENG. Reprinted from [147], © 2021 Elsevier Ltd All rights reserved. (e) The schematic diagram of three motion states. Reprinted from [148], © 2021 Elsevier Ltd All rights reserved. (f) Structure of the spherical W-TENG and enlarged view of one spiral TENG unit inside. [149] John Wiley & Sons. © 2022 Wiley-VCH GmbH. (g) The multilayered helical spring-like W-TENG. [150] John Wiley & Sons. © 2023 Wiley-VCH GmbH. (h) The magnets on the rotor and stator. Reprinted from [151], © 2022 Battelle Memorial Institute. Published by Elsevier Ltd. (i) The swing self-regulated W-TENG. [152] John Wiley & Sons. © 2023 Wiley-VCH GmbH.

4.4. Rotating structure

The rotating structure is also a common design, typically featuring one or more components that revolve around a central axis. When waves pass by, these components start to rotate. These components can either directly constitute the W-TENGs to generate output or transmit energy through a rotating shaft driven by their rotation. This rotation maintains stable energy output despite continuous wave fluctuations.

The advantage of W-TENGs composed of direct rotation of components is that they have a simple structure and can fully respond to wave disturbance. As shown in figure 10(a), Gao *et al* [153] proposed a gyroscope-structured W-TENG (GS-TENG), which installed two inner and outer power generation units through two mutually perpendicular central axes. When driven by water waves from random directions, the

GS-TENG's inner and outer power generation units could move freely in different directions. When the wave excitation disappeared, the reciprocating motion could continue due to the inertia of the eccentric ball. Feng *et al* [154] reported a cylindrical W-TENG that extended the rotation time by adjusting the filling and size of its rotating blades, as shown in figure 10(b). When the ratio of solid to hollow blades was 1:1, the W-TENG rotor, with the appropriate mass and barycenter position, exhibited the longest duration and best output performance. By adjusting the outer diameter of the rotor, there was a small air gap between the rotor and the external fixed electrodes to ensure that it could rotate for a long time while being powered. As shown in figure 10(c), Wang *et al* [155] designed a three-phase multi-group W-TENG. The three-phase W-TENG had three rotors, and the multi-group meant that each rotor was connected with multiple groups

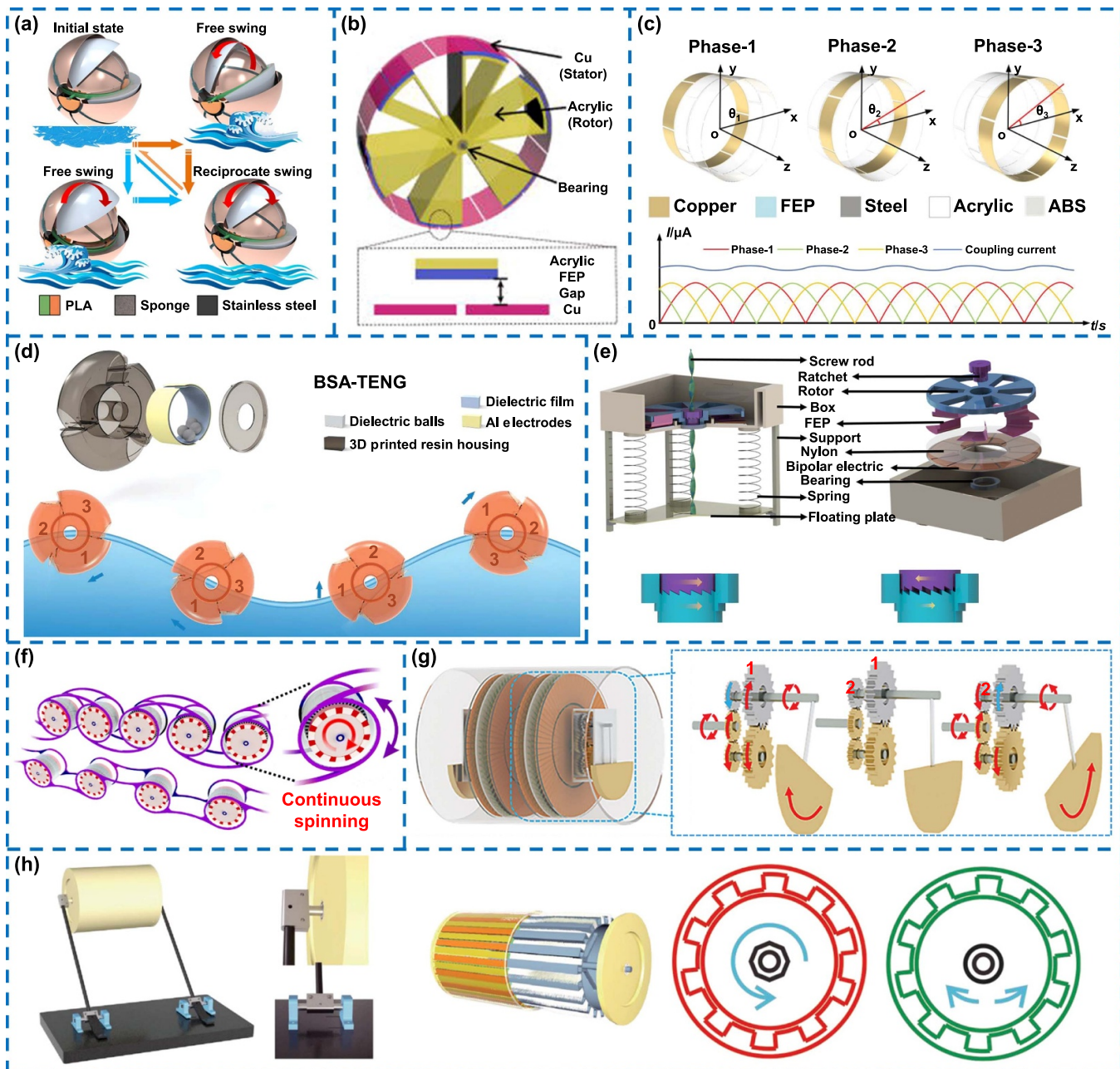


Figure 10. The rotating structure W-TENGs. (a) The gyroscope-structured W-TENG. Reprinted (adapted) with permission from [153]. Copyright (2022) American Chemical Society. (b) The schematic illustration of the cylindrical W-TENG. Reprinted from [154], with the permission of AIP Publishing. (c) The structure and output of the three-phase multi-group W-TENG. [155] John Wiley & Sons. © 2020 WILEY-VCH Verlag GmbH & Co. KGaA, Weinheim. (d) The barycenter self-adapting W-TENG. [156] John Wiley & Sons. © 2022 Wiley-VCH GmbH. (e) The section and partial exploded view of the W-TENG. Adapted from [157] with permission from the Royal Society of Chemistry. (f) The unidirectional continuous spinning W-TENG. Adapted from [158] with permission from the Royal Society of Chemistry. (g) The self-adaptive rotating W-TENG. [159] John Wiley & Sons. © 2023 Wiley-VCH GmbH. (h) The wave-driven linkage mechanism W-TENG. [160] John Wiley & Sons. © 2022 Wiley-VCH GmbH.

of electrodes in parallel. By adjusting the electrode angles, the W-TENG could produce a current output with almost the same frequency, equal amplitude and initial phase delay. It was worth noting that the superposition of rectified currents in each phase could produce an almost constant current with a low crest factor. They concluded the following rules: increasing the number of phases could obtain a DC output with a

lower crest factor, and increasing the number of groups could improve the total output performance.

While manufacturing the rotating components directly as the motion unit of W-TENGs is convenient, it also limits the type of power generation. Therefore, researchers are exploring various mechanical designs to transmit rotation to subsequent mechanisms, obtaining diverse motion characteristics

to meet different engineering needs. The direction of the wave is random, but the determined rotation direction of this structure makes it easier to design the power generation device. As shown in figure 10(d), Yang *et al* [156] reported a barycenter self-adapting W-TENG that harvested low-frequency wave energy through a physical gravity-guided structure. Waves entered the 3D printed resin housing from the water inlet, and the liquid's center of gravity was transferred by opening and closing a one-way unidirectional commutable baffle, thereby achieving continuous one-way rotation. The central slip ring was then driven to rotate, causing relative sliding between the dielectric film and the dielectric balls to generate electrical output. In figure 10(e), Jiang *et al* [157] combined a screw rod and a ratchet into a rotating W-TENG to achieve positive energy accumulation and motion rectification of continuous excitation. This configuration allowed the screw rod to transform reciprocating linear motion into rotational movement while the ratchet's selective locking mechanism ensured rotation exclusively in the counterclockwise direction. Inspired by the Brownian motor motion, Qiu *et al* [158] designed a unidirectional continuous spinning W-TENG with a distributed network architecture. The chains were networked with a chiral linkage structure, as figure 10(f) shows. The chiral configuration could exert fluctuating torque on each device. It was designed to convert irregular wave excitation into internal unidirectional motion through the synergy of non-mirror network linkers and a ratcheting effect enabled by one-way bearings.

A limitation of the above design is that only half of the swing kinetic energy caused by the waves is utilized, leading to the dissipation of the remaining energy. Zhang *et al* [159] created a self-adaptive rotating W-TENG, which collected bidirectional swing kinetic energy through a compound pendulum and then converted it into a unidirectional rotation of the transmission shaft by a functional gear-set. Gear 1 acted as the driving gear when the pendulum swung clockwise. When the pendulum swung counterclockwise, gear 2 acted as the driving gear. Figure 10(g) shows that this design kept the output shaft rotating clockwise. The output shaft drove the unidirectional rotating W-TENG with an inner and outer ring structure to generate output. This structure achieved excellent output under relatively small wave pressure. In figure 10(h), Han *et al* [160] reported a wave-driven linkage mechanism W-TENG (WLM-TENG) that could directly convert wave potential energy into rotor kinetic energy. The WLM-TENG could achieve unidirectional rotation or reciprocating swing by installing different bearings. The WLM-TENG was fixed at a certain height above the water surface, and the internal rotor was connected to the floating plate touching the water surface through a T-shaped connector. The floating plate was limited so that it was not perpendicular to the water's surface, allowing it to move up and down with the rise and fall of the waves. The connecting rod transformed the up-and-down motion into the rotational movement of the rotor. When the rotor rotated, the wool could contact and rub with the FEP fixed in the stator to generate output. For devices that could rotate in both directions to collect energy, their output was often limited by the rotation speed. They must keep rotating continuously rather than only small reciprocating swings.

5. Marine application prospects

Various material selections and structural fabrications are all aimed at optimizing the performance of W-TENGs, thereby ensuring their widespread use. Only by meeting the actual needs can the development of W-TENGs be effectively advanced. It can be said that practical application represents the future of W-TENGs. In this section, we primarily focus on applications of W-TENGs that show prospects in the maritime field or can help alleviate the current environmental pollution and energy shortage problems. It includes large-scale energy harvesting, electrochemical production, ocean navigation support and environmental protection.

5.1. Large-scale energy harvesting

The most basic application scenario of W-TENGs is to harvest wave energy for the grid. Due to the typically small size of a single unit, large-scale energy harvesting needs the aggregation of multiple W-TENGs into a system. In figure 11(a), Jiang *et al* [161] reported a swing structure W-TENG consisting of a swing component and a cylindrical shell. They evaluated the conversion efficiency from wave energy to electrical energy and concluded that large-scale wave energy harvesting could be achieved by connecting a large number of W-TENG units into a network. As shown in figure 11(b), Tan *et al* [162] designed an elliptic cylindrical swing structure W-TENG (EC-TENG) with robust self-stability and anti-overturning capabilities. Even if overturned, it could continue to work without affecting the output due to its completely symmetrical structure. While planar structures were easier to cover on the ocean surface, EC-TENG networks could collect wave energy on a large scale. In figure 11(c), Liang *et al* [40] proposed a system process from a single W-TENG to networked energy harvesting, in which the overall performance could be improved through circuit management.

The above studies indicate that large-scale wave energy harvesting through networking is feasible, yet guidance on how to connect W-TENG units and the final networking form remains limited. As shown in figure 11(d), Xu *et al* [163] took the lead in studying the coupling behavior between W-TENG units. They first tested free-unit and linked-unit forms and found that the linked-unit form had better output than the free-unit form. Linkages enable units to maintain optimal orientation and facilitate the transfer of force and energy between units. Three different W-TENG connection methods were further characterized: a rigid plate connection that did not deform, an elastic strip connection that could deform to some extent, and a string connection that could freely deform without extension. Rigid connections could form internal constraints between units, resulting in higher output at low frequencies. In contrast, elastic and string connections were flexible connection methods, with slightly higher high-frequency output and good overall performance. For the first time, Liu *et al* [164] conducted a strategy analysis on large-scale W-TENG networks and proposed four fundamental forms of electrical networking topology. A comprehensive study and comparison of these forms revealed that the configuration depicted in figure 11(e) yielded

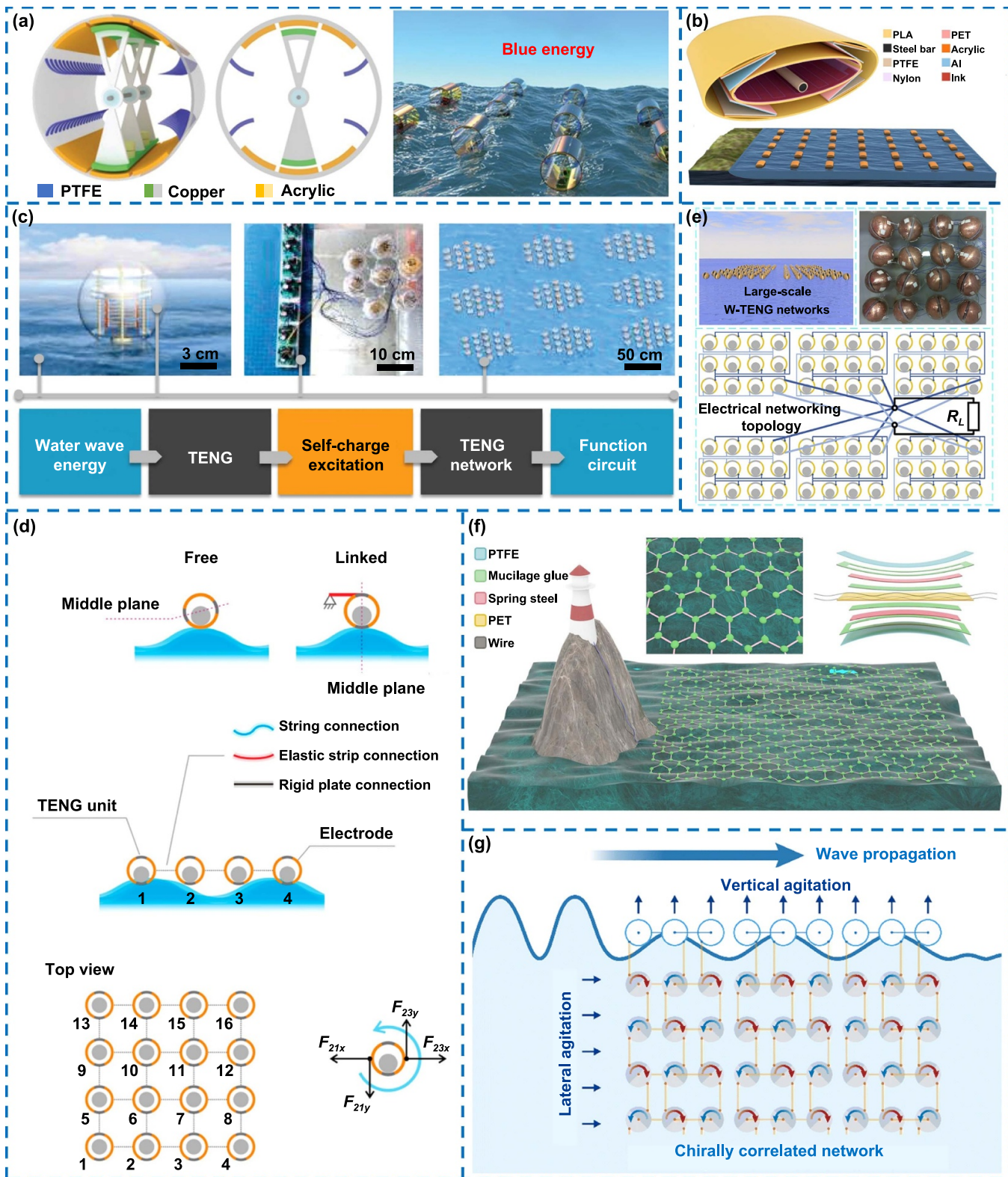


Figure 11. The large-scale energy harvesting of W-TENGs. (a) The swing-structure W-TENG and the system. [161] John Wiley & Sons. © 2020 WILEY-VCH Verlag GmbH & Co. KGaA, Weinheim. (b) The elliptic cylindrical swing structure W-TENG and the network. Reproduced from [162]. CC BY 4.0. (c) The system processes from a single W-TENG to networked energy harvesting. [40] John Wiley & Sons. © 2020 Wiley-VCH GmbH. (d) The coupling behavior between W-TENG units. Reprinted (adapted) with permission from [163]. Copyright (2018) American Chemical Society. (e) The strategy analysis on large-scale W-TENG networks. Reproduced with permission from [164]. CC BY-NC-ND 4.0. (f) The honeycomb connection topology of W-TENG. Reprinted from [165], © 2020 Elsevier Ltd All rights reserved. (g) The 3D chiral network of W-TENG. Adapted from [166] with permission from the Royal Society of Chemistry.

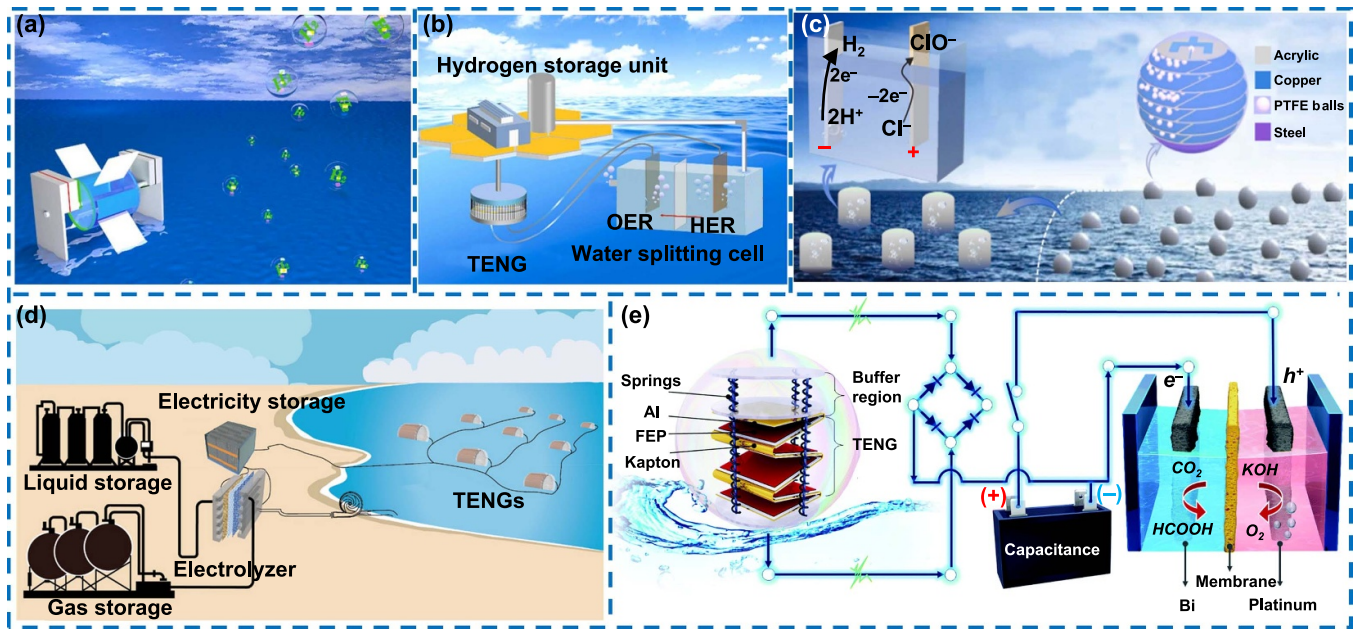


Figure 12. The applications of electrochemical production. (a) The pulsed cylindrical W-TENG used to generate hydrogen. Reprinted from [167], © 2021 Published by Elsevier Ltd. (b) The half-wave rectifying water flow-driven TENG. Reprinted from [110], © 2021 Elsevier Ltd All rights reserved. (c) The W-TENG with a self-controlled switch used to generate hydrogen. Reprinted from [61], © 2023 Elsevier Ltd All rights reserved. (d) The self-powered electrochemical system. [41] John Wiley & Sons. © 2021 Wiley-VCH GmbH. (e) The W-TENG to supply energy to produce formic acid. Adapted from [168] with permission from the Royal Society of Chemistry.

higher efficiency with fewer cables required. Although flexible connections performed well, the continuous undulations of the ocean surface could easily cause entanglement, affecting normal operation. Liu *et al* [165] solved this problem by connecting W-TENG units into a honeycomb connection topology through specially designed cables as shown in figure 11(f). The cable was made of spring steel tapes and three polymer films bonded together, transmitting electrical energy while placing fewer restrictions on the W-TENG unit. The W-TENG units were placed on connection points and could deflect and move both vertically and horizontally. The honeycomb topology allowed the overall structure to maintain its shape against external forces. Yang *et al* [139] achieved a self-assembly W-TENG network characterized by high autonomy and mechanical robustness through self-adaptive magnetic joints. The design was self-healing and easily reconfigurable, making it easy to adapt to the marine environment and avoid fatigue failure of the connected structure.

Currently, most topological networks are arranged above the water surface, occupying a large amount of ocean area and wasting its 3D space. Li *et al* [166] reported a 3D chiral network of W-TENG that could be configured to harvest wave energy from all directions at different scales and depths. The arrangement of large-scale 3D chiral W-TENG networks could serve as ocean power stations, as shown in figure 11(g). The network absorbed the mechanical energy from water wave propagation and stirred the rotation of the W-TENG unit through chiral coupling to generate electrical energy. Local agitations could also propagate within the network when the network was large enough. This work was a deep paradigm shift from mechanical metamaterial designs to

energy harvesting networks, providing a new idea for designing other harvesting networks.

5.2. Electrochemical production

If the electric energy generated by W-TENGs is consumed directly in the ocean, energy loss will be reduced. Ocean electrochemical production, as an innovative technology, shows great potential and broad application prospects. Therefore, many researchers use W-TENGs as power sources to conduct electrochemical production directly in the ocean.

Hydrogen is a clean energy source that only produces water after burning. The current efficient way to produce hydrogen is to electrolyze water. Consequently, researchers consider using W-TENGs as *in-situ* power sources to produce hydrogen using seawater resources. In figure 12(a), Zhu *et al* [167] designed a pulsed cylindrical W-TENG that could rotate driven by water or wind to generate electrical energy. When charged to 12 V, the $470 \mu\text{F}$ capacitor facilitated hydrogen gas generation through the electrolysis of a 3.5% sodium chloride solution. As shown in figure 12(b), Li *et al* [110] fabricated a half-wave rectifying water flow-driven W-TENG and obtained a DC output with large voltage and low loss. When the device reached 140 rpm, the hydrogen production rate was $12.32 \mu\text{l}\cdot\text{min}^{-1}$. The system's hydrogen energy conversion efficiency reached 2.38%. Zhang *et al* [61] designed a W-TENG with a self-controlled switch that could instantly discharge at ultrahigh instantaneous output power to achieve efficient hydrogen production. The integrated W-TENG charged a $470 \mu\text{F}$ capacitor to 5 V in 200 s, achieving a hydrogen production rate of approximately $64.5 \mu\text{l}\cdot\text{min}^{-1}$ under water wave

conditions. As shown in figure 12(c), this system converted electrical energy into chemical energy, with an energy conversion efficiency of 40.4%. In figure 12(d), Feng *et al* [41] proposed a self-powered electrochemical system from blue energy to green resources. The system stores the electrical energy converted by the W-TENG network in an electricity storage module, subsequently used for electrochemical reactions to produce hydrogen and other products. The system's energy conversion efficiency from electrical energy to chemical energy could reach 44.3%. The other products, such as chlorine and hypochlorite, are also of high value and can be used to remove pollutants, reflecting their potential in the field of environmental protection. In addition to hydrogen, hypochlorite and other products, Leung *et al* [168] used W-TENGs to supply energy to the reduction reaction of the CO₂ (CO₂RR) system to produce formic acid. Figure 12(e) shows a detailed schematic diagram of the wave-energy-driven CO₂RR system. The system included W-TENG, rectification and energy storage circuits, and two-electrode electrochemical cells for CO₂RR and oxygen evolution reaction. Under ideal conditions, the system could produce 2.798 μmol of formic acid per day using W-TENG from an area of 0.04 m². Although slower, the device successfully produced formic acid in actual ocean conditions, marking a breakthrough for practical applications. This work not only converted CO₂ into convenient storage and transportation fuel but also achieved CO₂ storage, making outstanding contributions to environmental protection.

5.3. Ocean navigation support

The most crucial equipment in the marine field includes various ships in navigation, and W-TENGs are developed for ocean navigation support. These developments can significantly contribute to maritime navigation lighting, precise positioning, and ship protection.

When a ship is sailing in the ocean, navigation lights, buoys, etc, can provide directional guidance for the ship. W-TENGs were designed to power navigation lights and buoys to ensure their long-term operation in the marine environment [169]. Xu *et al* [58, 62, 141] arrayed TENG units in buoys and continuously broke through the power density. Furthermore, W-TENGs could power ocean sensors to collect and transmit information, including water level monitoring [170–173], seawater status [174–176], and ship position [177]. Figure 13(a) shows the drawstring W-TENG (DS-TENG) designed by Zhao *et al* [178]. The DS-TENG could generate large-displacement motion under the dual action of waves and drawstrings to efficiently collect wave energy. Following energy management, the DS-TENG network could activate shallow water alarms and provide warnings to ships to avoid stranding. At the same time, they designed and manufactured a current-enhanced W-TENG (CE-TENG) using PTFE and nylon rollers spaced at intervals with interdigital electrodes [179]. As shown in figure 13(b), CE-TENG could power radar warning and play a significant role in ship collision avoidance. Chandrasekhar *et al* [180] developed a self-powered smart fishing net tracking buoy by fixing the smart buoy-TENG (SB-TENG) and

Bluetooth communication system on the fishing net. As shown in figure 13(c), the smartphone on fishing boats could control smart buoys on fishing nets through Bluetooth, triggering different LED lights to locate the fishing nets. Li *et al* [181] designed the liquid–solid contact W-TENG in buoys that could be used in a self-powered wireless SOS system. Figure 13(d) shows that the SOS distress signals could be transmitted in an emergency on a ship.

Ships and other ocean vehicles in contact with seawater are prone to biological adhesion and plant fouling. W-TENG's electrostatic induction can effectively solve this problem. Zhao *et al* [182] first proposed the use of electrostatic induction to change the potential for antifouling. They used the potential oscillation generated by an integrated triboelectric wave harvester (I-TEWH) designed to achieve antifouling on wetting insulation surfaces (figure 13(e)). The I-TEWH, based on triboelectric electrification at the solid–liquid interface, periodically pumped excess free electrons onto a conductive layer beneath the protected surface. This caused periodic changes in electrical potential near the surface to be protected, disrupting the inherent charge distribution of the microorganisms and preventing biofilm formation. The method was equally effective on a variety of organisms and species. In figure 13(f), Zhang *et al* [42] fabricated a liquid–solid W-TENG on the surface of a ship, using two ship steel plates as electrodes. A steel plate was coated with a dielectric material whose friction coefficient was about half lower than that of commercial marine anticorrosive coatings, and its ion adsorption effect was weak. The uncoated steel plate was positively charged and its ability to lose electrons was greatly reduced, thus maintaining anti-corrosion properties.

5.4. Environmental protection

It is mentioned many times in section 5.2 that W-TENGs provide support for environmental protection during electrochemical production. This section details some unique advancements W-TENGs have made in environmental protection.

As shown in figure 14(a), Zhou *et al* [43] reported a W-TENG-based self-powered AC electrocoagulation system that could treat organic pollutants in water. They utilized the AC generated by the contact–separation W-TENG, enabling the two Al electrodes to alternately serve as cathodes and anodes. When acting as an anode, Al³⁺ ions were alternately released from both sides of the electrode, reacting spontaneously with OH⁻ to generate the corresponding hydroxide, which adsorbed pollutants and induced coagulation. The flotation process of H₂ and O₂ bubbles produced when acting as a cathode could separate tiny particles in the solution. Ships inject or discharge ballast water to adjust stability based on cargo, with strict global regulations controlling this discharge. Because the quality of ballast water in different areas is different, random discharge will cause biological invasion. As shown in figure 14(b), Wang *et al* [183] designed a low-wear multilayer swing-structure W-TENG to provide power for ship ballast water monitoring. Ships could



Figure 13. The applications of ocean navigation support. (a) The drawstring W-TENG used to provide warnings to ships to avoid stranding. Adapted from [178], with permission from Springer Nature. (b) The CE-TENG that can provide power for radar warning. Reprinted from [179], © 2023 Elsevier Ltd All rights reserved. (c) The smart buoy-TENG toward self-powered smart fishing net tracker. Reprinted (adapted) with permission from [180]. Copyright (2020) American Chemical Society. (d) The liquid–solid contact W-TENG in buoys. [181] John Wiley & Sons. © 2018 WILEY-VCH Verlag GmbH & Co. KGaA, Weinheim. (e) The achieve antifouling on wetted insulating surfaces. [182] John Wiley & Sons. © 2016 WILEY-VCH Verlag GmbH & Co. KGaA, Weinheim. (f) The W-TENG used to ship anti-corrosion. Reprinted (adapted) with permission from [42]. Copyright (2022) American Chemical Society.

monitor the quality of ballast water and treat it as needed to protect the marine environment from damage. Moreover, this work achieved electrode hydration of a water-in-oil emulsion with a dehydration rate of 99.6%, which had potential application in treating marine oil spills. In response to the problem of excessive use of antibiotics causing residual pollution in the environment, Mo *et al* [184] prepared a self-powered photocatalytic system that could be used to remove tetracycline (figure 14(c-i)). The system was driven by a crowned W-TENG (C-TENG) integrated with 18 contact–separation mode units, as shown in figure 14(c-ii). The C-TENG not only realized the self-powered of the system, but also created an external electric field to enhance tetracycline removal efficiency. Specifically, the electric energy provided by C-TENG was rectified to form a potential difference between the two electrodes (figure 14(c-iii)). The electron–hole recombination rate of MIL-100(Fe) during the photocatalytic reaction

was reduced, thereby improving the photocatalytic degradation efficiency of tetracycline. Figure 14(c-iv) illustrates the principle of tetracycline removal.

The most pressing environmental issue today is carbon emissions, and we hope to achieve a carbon balance, that is, net-zero carbon or even negative carbon emissions (figure 14(d-i)). Xu *et al* [185] innovatively pumped CO₂ gas into W-TENG, enhancing their output and simultaneously reducing or offsetting carbon emissions. The manufacturing process, as shown in figure 14(d-ii), is simple and conducive to mass production. The encapsulated W-TENGs were connected through wires and transported to the ocean for network deployment. As shown in figure 14(d-iii), the high air pressure of the encapsulated CO₂ balanced the deep-sea water pressure while suppressing air breakdown. Increasing the air pressure also could enhance the breakdown strength. The authors conducted a detailed lifecycle assessment of the environmental

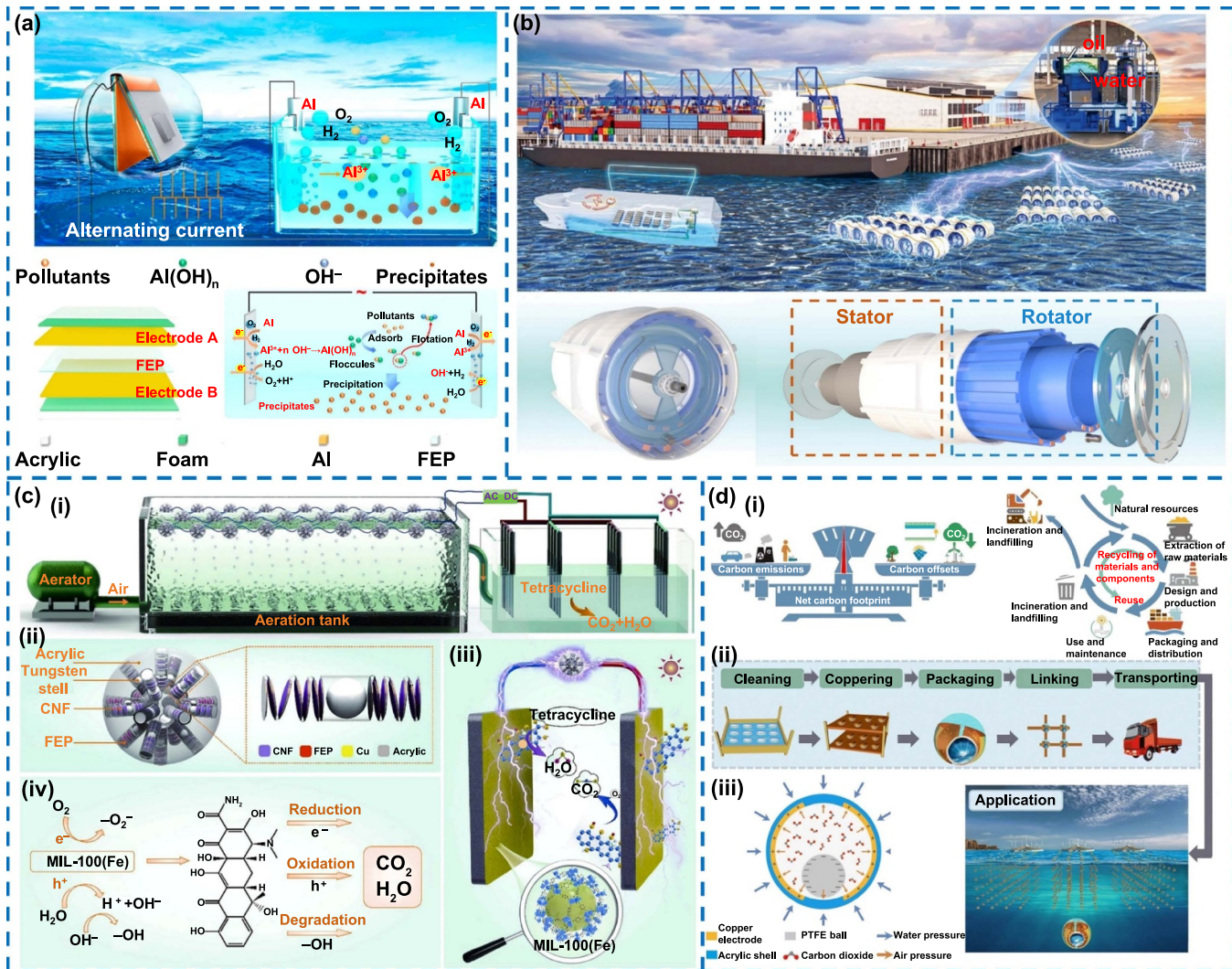


Figure 14. The applications of environmental protection. (a) The W-TENG-based self-powered AC electrocoagulation system. Reprinted (adapted) with permission from [43]. Copyright (2021) American Chemical Society. (b) The ship ballast water monitoring and electrode hydration. [183] John Wiley & Sons. © 2023 Wiley-VCH GmbH. (c) The self-powered photocatalytic system used to remove tetracycline. Reprinted from [184], © 2021 Elsevier Ltd All rights reserved. (d) The W-TENG used to control carbon emissions. Adapted from [185] with permission from the Royal Society of Chemistry.

status and carbon footprint of W-TENG. The carbon footprint distribution of W-TENG with and without encapsulated CO₂ was compared. Assuming that the W-TENGs could operate for ten years, in the case of no CO₂ charging, the carbon emission was 740 kg·m⁻³. However, after CO₂ charging, the carbon emissions could reach ~43 400 kg·m⁻³. At the same time, the W-TENGs were compared with other energy collectors. On average, the W-TENGs emit only 42 g of CO₂ per kW per h. These findings fully confirm that using W-TENGs to reduce carbon emissions is worth implementing.

In order to clearly evaluate current applications, in table 1, we have compiled and compared the typical structures of W-TENGs and traditional EMG devices [186–192]. As can be seen from table 1, W-TENGs have significant advantages in terms of volume, as it occupies a small ocean area. Moreover, although W-TENGs lack weight data, their structures generally do not contain ferromagnetic structures, so their mass is small. These advantages allow it to be deployed quickly in the

ocean. Additionally, EMGs have complex dynamic sealing, and the metal components are prone to rusting, potentially destroying the device. Due to their compact size, W-TENGs are easily waterproofed and sealed, and some liquid–solid mode devices can be directly deployed in seawater. Therefore, W-TENGs have strong environmental adaptability and can easily ensure longer operating time. Of course, EMGs still have obvious advantages in terms of output performance. In this regard, W-TENGs need to make up for this shortcoming through reasonable array design.

6. Summary and perspective

6.1. Summary

In this paper, the advancements in W-TENGs from materials manufacturing and structural fabrications to applications are comprehensively reviewed. It offers an exhaustive overview of

Table 1. Summary and comparison of some typical W-TENGs and traditional EMG devices.

Method	Structure	Volume	Weight	Perk of the Output	Environmental adaptability	Applications	References
TENG	Multi-layer structure	864 cm ³	—	1.15 MW·km ⁻² (Average)	Highly anticorrosive to the marine environment	Large-scale blue energy harvesting	[39]
TENG	Multi-layer structure	1.8 × 10 ⁻⁴ m ³	—	1.28 mW	—	Large-scale energy harvesting	[163]
TENG	Channel structure	1.17 × 10 ⁻² m ³	—	80.29 W·m ⁻³	Treated with waterproof glue to avoid the adverse effects of humidity	The utilization of ocean blue energy	[143]
TENG	Elastic structure	4.19 × 10 ⁻³ m ³	—	1.1 W·m ⁻²	Waterproofed with silicone sealant	Meeting the daily power needs encountered in marine applications	[84]
TENG	Elastic structure	3.14 × 10 ⁻⁵ m ³	—	57.3 mW·cm ⁻³	Encapsulated to avoid contamination or water soaking	Corrosion prevention for stainless steel in the marine environment	[89]
TENG	Rotating structure	2.8 × 10 ⁻⁴ m ³	—	218.2 W·m ⁻³	—	Sustainable power supply for small electronic products	[33]
TENG	Multi-layer structure	904.78 cm ³	—	10 mW	Sealed with epoxy paint	Self-powered environmental monitoring and hydrological research	[36]
EMG	Point-absorber	—	2.4 kg(Buoy mass)	14 W	—	Powering the sensors in the satellite-respondent buoy	[186]
EMG	Gyroscopic	0.45 m ³	90 kg(Float mass)	138.56 W	—	Expanding the application scenario of wave gliders	[187]
EMG	Pendulum	1 508 cm ³	5 kg(Pendulum mass)	0.3 W (Average)	Installed inside the hull	Extending the work time of underwater mooring platforms	[188]
EMG	Serial four-bar linkage	Width 3.4 m length 1.63 m	25 kg(Body included)	2.6 W	—	Enhancement of endurance capability of ocean robots	[189]
EMG	Point-absorber	0.034 m ³	—	5.49 W (Average)	Covered with an acrylic plate, coated with glass	Powering wireless sensors used in sea-crossing bridges	[190]
EMG	Point-absorber	0.149 m ³	—	63 W (Average)	Good combination of weldability and resistance to saltwater	Lay the foundation for the research of new wave energy converters	[191]
EMG	Point-absorber	0.452 m ³	78 kg(Buoy mass)	74.8 W (Average)	—	Large wave energy plant	[192]

the current developments and endeavors across various aspects of W-TENGs, highlighting their potential for efficient maritime utilization. The review of typical research on W-TENGs focuses on the following three areas: materials, structures, and applications. However, it needs to be noted that each study is often not limited to the new results in only one of the above three areas. The reported results may involve multiple areas and are thus inherently interrelated. The detailed parameters

of some typical W-TENGs are summarized and compared in table 2.

The basic principle and fundamental working modes of TENG demonstrate the reliability of its energy conversion and the scalability of its structural design. There is currently a relatively clear scientific explanation of the basic principle of triboelectricity, which reveals the charge transfer process during contact and separation between different materials. However,

Table 2. Summary and comparison of the detailed parameters of some typical W-TENGs.

Structure	Mode	Triboelectric material	Materials treatment	Perk of the Output	Working conditions	Applications	References
Multi-layer structure	Rolling mode	Kapton, NSP-Al	Chemical modification	580 V 23.5 μ A	1–2 Hz	Large-scale energy harvesting	[103]
	Single-electrode mode	PTFE-Cu	Etching nanowire array	28 μ W	Wave	Self-powered hydrological monitoring system	[106]
	Vertical contact– separation mode	FEP-Cu	Inductive coupled plasma	13.2 mW·m ⁻² (Average)	1–5 Hz	Ocean navigation support	[132]
	Vertical contact– separation mode	PTFE-Cu	Stretching treatment is applied for the raw PTFE film.	9.559 W·m ⁻³	1–2 Hz	Ocean information monitoring and power to islands	[145]
	Vertical contact– separation mode	FEP-Cu	Injected electrons through corona discharge technology	8.5 mW	0.5–2 Hz	Self-charging power pack	[146]
Channel structure	Vertical contact– separation mode	Water, PMMA	Fluorine-containing materials were added to the acrylic resin	2.83 mW·m ⁻²	3 Hz	Ocean energy collection and self-powered sensing	[125]
	Rolling mode	PTFE-conductive ink & PTFE-Al	Inductive coupled plasma	8.3 mW	0.25–1.25 Hz	Large-scale energy harvesting	[162]
	Rolling mode	Silicone rubber-Ag-Cu	Ultraviolet (UV) treatment and fabricating microstructures	0.128 mW	1.25–5 Hz	Large-scale energy harvesting	[163]
Elastic structure	Vertical contact– separation mode	FEP-Cu	Ionized charges are pre-implanted through corona discharging process	0.67 mW·cm ⁻³		Broad energy harvesting	[117]
	Vertical contact– separation mode	CNF/TMS, FEP-Cu	Interfacial modification	38.72 μ W	1.5 Hz	Scalable distributed energy harvesting	[120]
	Vertical contact– separation mode	Calcium Alginate-Al	New materials preparation	9.5 μ W	1–4 Hz	Environmental protection	[124]
	Vertical contact– separation mode	PTFE-Al	New materials preparation	14.7 mW	0.85–2.65 Hz	Ocean navigation support	[148]
Rotating structure	Vertical contact– separation mode	FEP, Nylon-Al	Chemically etched nylon films	12 V	0.17–1.25 Hz	Large-scale energy harvesting	[118]
	Freestanding triboelectric-layer mode	FEP-Cu	Micro/nano surface structure of the FEP film	45.18 mW·kg (Average)	0.5–1.5 Hz	Powering marine Internet of Things nodes	[159]
	Freestanding triboelectric-layer mode	PTFE, Acrylic-Cu	Electrons were pre-injected by the corona discharging method	4.56 mW	0.8–1.5 Hz	Self-powered sensing and monitoring	[161]

detailed theoretical formulas and quantitative descriptions are yet to be further explored, limiting the precise interpretation of experimental data and the reasonable prediction of subsequent evolution processes. Secondly, the basic materials manufacturing of W-TENGs, including mainly the in-depth analysis of materials selection, contact optimization, chemical treatment and new materials preparation are then summarized. It is widely realized that triboelectric materials are the core issues of W-TENGs, deserving a wider selection of materials and unified standards for quantifying. Addressing specific requirements, the preparation of the new materials emerges as the most dependable strategy. This underscores the critical influence of materials science in enhancing the performance of the W-TENGs. In our analysis of the structural fabrication of W-TENGs, we categorize the common configurations and thoroughly explore the design concepts of multi-layer structures, channel structures, elastic structures and rotating structures. The primary objective in the structural fabrication of W-TENGs is to formulate designs that offer efficient responses to wave excitation while maintaining the structure's stability and longevity within a dynamic marine environment. Achieving this balance facilitates the realization of high power density and superior energy efficiency. Lastly, the application prospects of W-TENGs in the marine field are explored. Beyond its significant capacity for large-scale energy harvesting for power supply, W-TENGs have also realized innovative functions in electrochemical production, ocean navigation support, and environmental protection. In summary, as an evolving technology, W-TENGs have achieved exciting progress in sustainable energy and marine applications, positioning it as a focal area for forthcoming research endeavors.

6.2. Perspective

Based on the review of the W-TENGs, this section provides an in-depth analysis and perspectives on the future development in this research field. We discuss in detail the potential advancements of W-TENGs in materials manufacturing, structural design, system optimization, and practical application promotion. At the same time, targeted solution strategies and suggestions are pointed out. The specific perspectives are as follows:

1. In theories: to enhance the efficiency and practicality of the TENGs, theoretical research must be further deepened. Establishing a quantitative relationship between TENGs' output performance and critical factors such as materials properties, design parameters and environmental conditions is imperative. This process requires the integration of rigorous and systematic theoretical derivation with experimental and simulation results to elucidate the intricate interplay among these factors. On this basis, a comprehensive performance evaluation system for TENGs should be developed. This system can provide standardized indicators such as energy conversion efficiency, stability and environmental adaptability. It can be used to measure whether TENGs can meet the conditions of extreme manufacturing

methods and their survivability in complex environments. Based on the above research, a thorough evaluation and comparison of various TENG models and designs can be conducted, facilitating their continual refinement and advancement.

2. In materials: the selection process for triboelectric materials must be standardized rather than based on random attempts. It is necessary to use standardized methods to measure the triboelectric properties of the existing materials and to formulate triboelectric sequence tables under various environmental conditions. In addition, other properties of materials, such as strength, stiffness, elasticity, need to be studied further. There is a crucial need to synchronize with advances in materials science, focusing on developing new materials manufactured for specific requirements. This involves integrating existing theoretical knowledge in the materials preparation process to validate the accuracy of these theories. While ensuring demand and output performance, environmental protection and sustainability requirements should also be realized. For both the existing materials and new materials, their reusability, pressure resistance, and temperature range determine the breadth and depth of W-TENGs applications.
3. In structures: for the structural design and fabrication of W-TENGs, the current practice mainly relies on early research and integration with unique mechanical structures for enhancement. To boost W-TENGs' energy collection efficiency and their suitability for marine environments, an in-depth mechanical analysis of their structures must be performed. Based on marine engineering mechanics, detailed research is conducted in aspects such as fluid dynamics, structural dynamics and materials mechanics. Special attention must be given to the complex coupling effect between the W-TENG's internal mechanics and the external wave excitation. A comprehensive and systematic approach is essential for structural optimization. The sensory capabilities of TENGs offer the potential for creating an adaptive control system for W-TENGs, where the TENG acts as both a power generator and a sensor. Specifically, this system can achieve effective energy conversion while monitoring and evaluating the operating status of the W-TENGs itself. It is necessary to develop efficient algorithms based on preliminary structural dynamics analysis and research on electrical output characteristics, which can accurately identify and respond to environmental changes. By adjusting the structural configuration or operating parameters of W-TENGs, such as adjusting the draft or the moment of inertia of the floating body, etc, this system can play an important role in maintaining the optimal balance between structural stability and power generation efficiency in practical applications. For structures, there is also a very critical basic research that needs to be conducted, which is to propose a standard (and commonly recognized) definition of the 'power density' concept. This involves providing the volume of the power take-off unit and normalizing the output with incident wave parameters (i.e. wave height and wave frequency). This will probably give rise to a 'power density curve' or 'power density contour'.

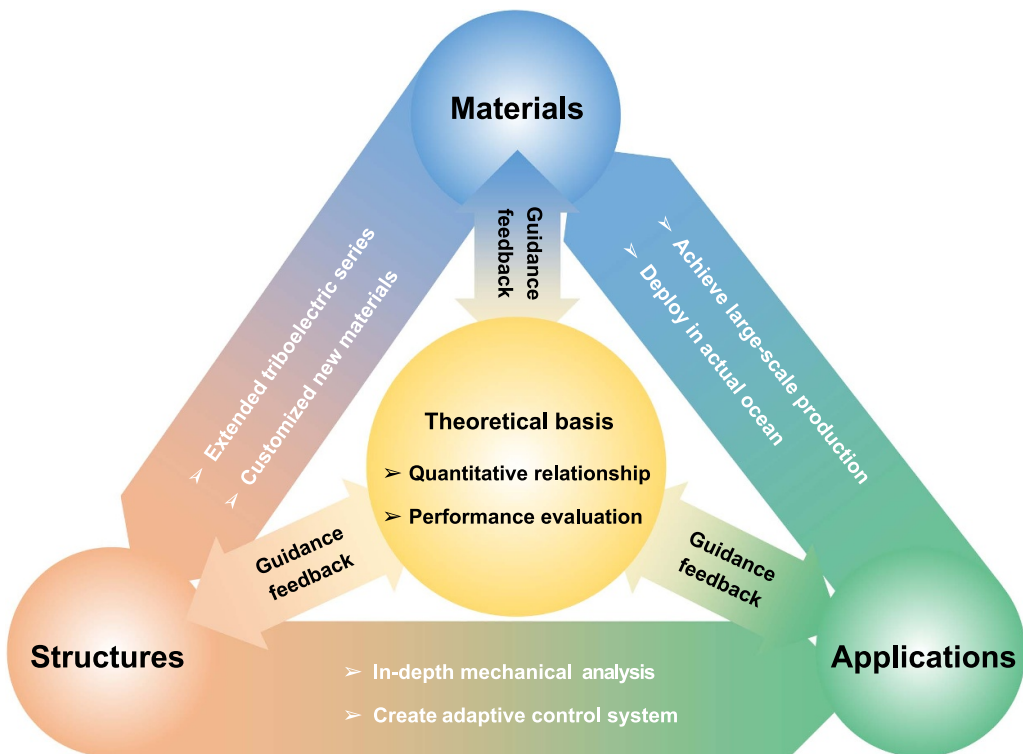


Figure 15. Future perspectives and development directions of W-TENGs.

4. In applications: the production of W-TENGs is currently mainly based on customized designs, which can meet the needs of experimental testing, but is far away from practical application. Therefore, it is necessary to establish a standardized process for materials manufacturing and structural fabrication of W-TENGs. Achieving large-scale production is essential to ensure both the affordability and quality of W-TENGs. After realizing the standardized production of W-TENGs, we should accelerate the application of W-TENGs to the actual marine environment. The actual problems should be fed back to the research and development stage. Neither experiments nor simulations can imitate the real application environment, and the data measured in actual applications have more guiding value. The output data of W-TENGs under actual sea conditions can be used to accurately evaluate the performance of materials and designs, and expand the scope of theoretical research. Special attention should be paid here to the conversion efficiency of W-TENGs in the actual environment. Additionally, analyzing the output characteristics can also guide the next step in designing efficient management circuits and expanding application fields. This is significantly different from basic buck rectification, threshold switch design and energy storage management. As for the applications, we suggest that the most valuable and easiest strategy to implement currently is to provide energy for marine IoT nodes.

Finally, the future perspectives and development directions of W-TENGs are visually displayed in figure 15. Progress in each direction will profoundly affect the rest. In this context,

improving the performance of the W-TENGs is a systematic project. We expect this comprehensive review to serve not only as a valuable reference for current researchers and engineers in the involved field but also to guide new researchers toward impactful contributions. Our aim is to advance the development of W-TENGs towards greater maturity and practicality.

Acknowledgments

This work was supported by the National Natural Science Foundation of China (Grant No. 52101382) and the National Key R&D Project from the Ministry of Science and Technology (Grant No. 2021YFA1201604), Application Research Program of Liaoning Province (Grant No. 2022JH2/101300219), the China Postdoctoral Science Foundation (Fellowship No. 2022M710570) and the China Scholarship Council (CSC No. 202306570038) for supporting the first author at The University of Western Australia as a visiting PhD student.

Conflict of interest

The authors declare that they have no conflict of interest.

ORCID iDs

Chuanqing Zhu  <https://orcid.org/0000-0003-0924-0660>
 Qijun Sun  <https://orcid.org/0000-0003-2130-7389>
 Minyu Xu  <https://orcid.org/0000-0002-3772-8340>

References

- [1] Parida B, Iniyian S and Goic R 2011 A review of solar photovoltaic technologies *Renew. Sustain. Energy Rev.* **15** 1625–36
- [2] Yang T, Chen W, Zhou K L and Ren M L 2018 Regional energy efficiency evaluation in China: a super efficiency slack-based measure model with undesirable outputs *J. Clean. Prod.* **198** 859–66
- [3] Kamarulzaman A, Hasanuzzaman M and Rahim N A 2021 Global advancement of solar drying technologies and its future prospects: a review *Sol. Energy* **221** 559–82
- [4] Colelli F P, Emmerling J, Marangoni G, Mistry M N and De Cian E 2022 Increased energy use for adaptation significantly impacts mitigation pathways *Nat. Commun.* **13** 4964
- [5] Parker R W R, Blanchard J L, Gardner C, Green B S, Hartmann K, Tyedmers P H and Watson R A 2018 Fuel use and greenhouse gas emissions of world fisheries *Nat. Clim. Change* **8** 333–7
- [6] Eskander S M S U and Fankhauser S 2020 Reduction in greenhouse gas emissions from national climate legislation *Nat. Clim. Change* **10** 750–6
- [7] Udeagha M C and Muchapondwa E 2023 Striving for the United Nations (UN) sustainable development goals (SDGs) in BRICS economies: the role of green finance, fintech, and natural resource rent *Sustain. Dev.* **31** 3657–72
- [8] Hassan A, Ilyas S Z, Jalil A and Ullah Z 2021 Monetization of the environmental damage caused by fossil fuels *Environ. Sci. Pollut. Res.* **28** 21204–11
- [9] Morss R E, Wilhelmi O V, Meehl G A and Dilling L 2011 Improving societal outcomes of extreme weather in a changing climate: an integrated perspective *Annu. Rev. Environ. Resour.* **36** 1–25
- [10] Manosalidis I, Stavropoulou E, Stavropoulos A and Bezirtzoglou E 2020 Environmental and health impacts of air pollution: a review *Front. Public Health* **8** 14
- [11] Proskuryakova L 2018 Updating energy security and environmental policy: energy security theories revisited *J. Environ. Manage.* **223** 203–14
- [12] Chen F Z, Duic N, Alves L M and Da Graça Carvalho M 2007 Renewislands—renewable energy solutions for islands *Renew. Sustain. Energy Rev.* **11** 1888–902
- [13] Martí L and Puertas R 2022 Sustainable energy development analysis: energy trilemma *Sustain. Technol. Entrep.* **1** 100007
- [14] Fang Y, Tang T Y, Li Y F, Hou C, Wen F, Yang Z, Chen T, Sun L N, Liu H C and Lee C 2021 A high-performance triboelectric-electromagnetic hybrid wind energy harvester based on rotational tapered rollers aiming at outdoor IoT applications *iScience* **24** 102300
- [15] Liu S C, Liu X, Zhou G L, Qin F X, Jing M X, Li L, Song W L and Sun Z Z 2020 A high-efficiency bioinspired photoelectric-electromechanical integrated nanogenerator *Nat. Commun.* **11** 6158
- [16] Salter S H 1974 Wave power *Nature* **249** 720–4
- [17] Barnier B, Domina A, Gulev S, Molines J M, Maitre T, Penduff T, Le Sommer J, Brasseur P, Brodeau L and Colombo P 2020 Modelling the impact of flow-driven turbine power plants on great wind-driven ocean currents and the assessment of their energy potential *Nat. Energy* **5** 240–9
- [18] Hu H K, Xue W D, Jiang P and Li Y 2022 Bibliometric analysis for ocean renewable energy: an comprehensive review for hotspots, frontiers, and emerging trends *Renew. Sustain. Energy Rev.* **167** 112739
- [19] Ellabban O, Abu-Rub H and Blaabjerg F 2014 Renewable energy resources: current status, future prospects and their enabling technology *Renew. Sustain. Energy Rev.* **39** 748–64
- [20] Henfridsson U, Neimane V, Strand K, Kapper R, Bernhoff H, Danielsson O, Leijon M, Sundberg J, Thorburn K and Ericsson E 2007 Wave energy potential in the Baltic Sea and the Danish part of the North Sea, with reflections on the Skagerrak *Renew. Energy* **32** 2069–84
- [21] López I, Andreu J, Ceballos S, Alegría I M D and Kortabarria I 2013 Review of wave energy technologies and the necessary power-equipment *Renew. Sustain. Energy Rev.* **27** 413–34
- [22] De O. Falcão A F 2010 Wave energy utilization: a review of the technologies *Renew. Sustain. Energy Rev.* **14** 899–918
- [23] Langhamer O, Haikonen K and Sundberg J 2010 Wave power—sustainable energy or environmentally costly? A review with special emphasis on linear wave energy converters *Renew. Sustain. Energy Rev.* **14** 1329–35
- [24] Göteman M, Giassi M, Engström J and Isberg J 2020 Advances and challenges in wave energy park optimization—a review *Front. Energy Res.* **8** 26
- [25] Iglesias G, López M, Carballo R, Castro A, Fraguera J A and Frigaard P 2009 Wave energy potential in Galicia (NW Spain) *Renew. Energy* **34** 2323–33
- [26] McCabe A P, Bradshaw A, Meadowcroft J A C and Aggidis G 2006 Developments in the design of the PS Frog Mk 5 wave energy converter *Renew. Energy* **31** 141–51
- [27] Zhang Y X, Zhao Y J, Sun W and Li J X 2021 Ocean wave energy converters: technical principle, device realization, and performance evaluation *Renew. Sustain. Energy Rev.* **141** 110764
- [28] Zhu C Q et al 2023 Highly integrated triboelectric-electromagnetic wave energy harvester toward self-powered marine Buoy *Adv. Energy Mater.* **13** 2301665
- [29] Rhinefrank K et al 2006 Novel ocean energy permanent magnet linear generator buoy *Renew. Energy* **31** 1279–98
- [30] Fan F R, Tian Z Q and Wang Z L 2012 Flexible triboelectric generator *Nano Energy* **1** 328–34
- [31] Wang Z L 2017 Catch wave power in floating nets *Nature* **542** 159–60
- [32] Yang Y, Zhang H L, Liu R Y, Wen X N, Hou T C and Wang Z L 2013 Fully enclosed triboelectric nanogenerators for applications in water and harsh environments *Adv. Energy Mater.* **3** 1563–8
- [33] Wu S S, Yang J H, Wang Y F, Liu B, Xiong Y, Jiao H S, Liu Y, Bao R R, Wang Z L and Sun Q J 2023 UFO-shaped integrated triboelectric nanogenerator for water wave energy harvesting *Adv. Sustain. Syst.* **7** 2300135
- [34] Wang Y Z, Nazar A M, Wang J J, Xia K Q, Wang D L, Ji X S and Jiao P C 2021 Rolling spherical triboelectric nanogenerators (RS-TENG) under low-frequency ocean wave action *J. Mar. Sci. Eng.* **10** 5
- [35] Lone S A, Lim K C, Kaswan K, Chatterjee S, Fan K P, Choi D, Lee S, Zhang H L, Cheng J and Lin Z H 2022 Recent advancements for improving the performance of triboelectric nanogenerator devices *Nano Energy* **99** 107318
- [36] Wang X F, Niu S M, Yin Y J, Yi F, You Z and Wang Z L 2015 Triboelectric nanogenerator based on fully enclosed rolling spherical structure for harvesting low-frequency water wave energy *Adv. Energy Mater.* **5** 1501467
- [37] Gao W C, Shao J J, Sagee-Crentsil K and Duan W H 2021 Investigation on energy efficiency of rolling triboelectric nanogenerator using cylinder-cylindrical shell dynamic model *Nano Energy* **80** 105583
- [38] Yang W Z, Zhao T C, Zhou S N, Niu B, Tang C X, Yan J J, Hu C and Ma Y 2024 Experimental studies on particle

- dampers with energy harvesting characteristics *J. Vib. Eng. Technol.* **12** 2571–83
- [39] Chen J *et al* 2015 Networks of triboelectric nanogenerators for harvesting water wave energy: a potential approach toward blue energy *ACS Nano* **9** 3324–31
- [40] Liang X, Jiang T, Feng Y W, Lu P J, An J and Wang Z L 2020 Triboelectric nanogenerator network integrated with charge excitation circuit for effective water wave energy harvesting *Adv. Energy Mater.* **10** 2002123
- [41] Feng Y W, Han J J, Xu M J, Liang X, Jiang T, Li H X and Wang Z L 2022 Blue energy for green hydrogen fuel: a self-powered electrochemical conversion system driven by triboelectric nanogenerators *Adv. Energy Mater.* **12** 2103143
- [42] Zhang C G, Zhang B F, Yuan W, Yang O, Liu Y B, He L X, Zhao Z H, Zhou L L, Wang J and Wang Z L 2022 Seawater-based triboelectric nanogenerators for marine anticorrosion *ACS Appl. Mater. Interfaces* **14** 8605–12
- [43] Zhou L L, Liu L, Qiao W Y, Gao Y K, Zhao Z H, Liu D, Bian Z F, Wang J and Wang Z L 2021 Improving degradation efficiency of organic pollutants through a self-powered alternating current electrocoagulation system *ACS Nano* **15** 19684–91
- [44] Li X Y, Xu L and Wang Z L 2024 Networking strategies of triboelectric nanogenerators for harvesting ocean blue energy *Nanoenergy Adv.* **4** 70–96
- [45] Wang W L, Yang D F, Yan X R, Wang L C, Hu H and Wang K 2023 Triboelectric nanogenerators: the beginning of blue dream *Front. Chem. Sci. Eng.* **17** 635–78
- [46] Dip T M, Arin M R A, Anik H R, Uddin M M, Tushar S I, Sayam A and Sharma S 2023 Triboelectric nanogenerators for marine applications: recent advances in energy harvesting, monitoring, and self-powered equipment *Adv. Mater. Technol.* **8** 2300802
- [47] Jiang Y, Liang X, Jiang T and Wang Z L 2024 Advances in triboelectric nanogenerators for blue energy harvesting and marine environmental monitoring *Engineering* **33** 204–24
- [48] Zhang C, Zhao J Q, Zhang Z, Bu T Z, Liu G X and Fu X P 2023 Tribotronics: an emerging field by coupling triboelectricity and semiconductors *Int. J. Extrem. Manuf.* **5** 042002
- [49] Shi Q F, Sun Z D, Zhang Z X and Lee C 2021 Triboelectric nanogenerators and hybridized systems for enabling next-generation IoT applications *Research* **2021** 6849171
- [50] Wu M W, Zhu C Q, Liu X T, Wang H, Si J C, Xu M Y and Mi J C 2024 Recent advances in nanogenerators driven by flow-induced vibrations for harvesting energy *Mater. Today Energy* **41** 101529
- [51] Li Y M, Liu X, Ren Z W, Luo J J, Zhang C, Cao C Y, Yuan H and Pang Y K 2024 Marine biomaterial-based triboelectric nanogenerators: insights and applications *Nano Energy* **119** 109046
- [52] Yan J, Mei N, Zhang D P, Zhong Y H and Wang C 2022 Review of wave power system development and research on triboelectric nano power systems *Front. Energy Res.* **10** 966567
- [53] Zhang C G, Hao Y J, Yang J Y, Su W, Zhang H K, Wang J, Wang Z L and Li X H 2023 Recent advances in triboelectric nanogenerators for marine exploitation *Adv. Energy Mater.* **13** 2300387
- [54] Zhai H, Ding S, Chen X Y, Wu Y C and Wang Z L 2023 Advances in solid–solid contacting triboelectric nanogenerator for ocean energy harvesting *Mater. Today* **65** 166–88
- [55] Chen G Y, Xu L, Zhang P P, Chen B D, Wang G X, Ji J H, Pu X and Wang Z L 2020 Seawater degradable triboelectric nanogenerators for blue energy *Adv. Mater. Technol.* **5** 2000455
- [56] Wen X N, Yang W Q, Jing Q S and Wang Z L 2014 Harvesting broadband kinetic impact energy from mechanical triggering/vibration and water waves *ACS Nano* **8** 7405–12
- [57] Jiang T, Yao Y Y, Xu L, Zhang L M, Xiao T X and Wang Z L 2017 Spring-assisted triboelectric nanogenerator for efficiently harvesting water wave energy *Nano Energy* **31** 560–7
- [58] Xu M Y, Zhao T C, Wang C, Zhang S L, Li Z, Pan X X and Wang Z L 2019 High power density tower-like triboelectric nanogenerator for harvesting arbitrary directional water wave energy *ACS Nano* **13** 1932–9
- [59] Zhang Z Y, Hu Z Y, Wang Y, Wang Y W, Zhang Q Q, Liu D H, Wang H and Xu M Y 2022 Multi-tunnel triboelectric nanogenerator for scavenging mechanical energy in marine floating bodies *J. Mar. Sci. Eng.* **10** 455
- [60] Chen X W, Bao G W, Xie S X, Qin X H and Wang J Q 2023 A self-powered wide-range ocean-wave sensor enabled by triboelectric nanogenerators embedded with overrunning clutches *Nano Energy* **115** 108685
- [61] Zhang W, He W C, Dai S G, Ma F X, Lin P, Sun J L, Dong L and Hu C G 2023 Wave energy harvesting based on multilayer beads integrated spherical TENG with switch triggered instant discharging for self-powered hydrogen generation *Nano Energy* **111** 108432
- [62] Wang H *et al* 2021 Sandwich-like triboelectric nanogenerators integrated self-powered buoy for navigation safety *Nano Energy* **84** 105920
- [63] Jiang Q W, Jie Y, Han Y, Gao C Z, Zhu H R, Willander M, Zhang X J and Cao X 2015 Self-powered electrochemical water treatment system for sterilization and algae removal using water wave energy *Nano Energy* **18** 81–88
- [64] Guo H Y, Yeh M H, Zi Y L, Wen Z, Chen J, Liu G L, Hu C G and Wang Z L 2017 Ultralight cut-paper-based self-charging power unit for self-powered portable electronic and medical systems *ACS Nano* **11** 4475–82
- [65] Wang Z L and Wang A C 2019 On the origin of contact-electrification *Mater. Today* **30** 34–51
- [66] Xu C *et al* 2018 On the electron-transfer mechanism in the contact-electrification effect *Adv. Mater.* **30** 1706790
- [67] Luo J J and Wang Z L 2020 Recent progress of triboelectric nanogenerators: from fundamental theory to practical applications *EcoMat* **2** e12059
- [68] Wang X Y, Zhu C Q, Wu M W, Zhang J L, Chen P F, Chen H, Jia C X, Liang X and Xu M Y 2022 A novel flow sensing and controlling system based on the flapping film triboelectric nanogenerator toward smart factories *Sens. Actuators A* **344** 113727
- [69] Guo X Y *et al* 2024 Boosting free-rotating disk triboelectric nanogenerator through alcohol-soluble nylon film, preventing air breakdown *ACS Appl. Electron. Mater.* **6** 376–85
- [70] Zhao Z Q *et al* 2022 An array of flag-type triboelectric nanogenerators for harvesting wind energy *Nanomaterials* **12** 721
- [71] Wang Y, Yang E, Chen T Y, Wang J Y, Hu Z Y, Mi J C, Pan X X and Xu M Y 2020 A novel humidity resisting and wind direction adapting flag-type triboelectric nanogenerator for wind energy harvesting and speed sensing *Nano Energy* **78** 105279
- [72] Zou Y J *et al* 2022 A high-performance flag-type triboelectric nanogenerator for scavenging wind energy toward self-powered IoTs *Materials* **15** 3696
- [73] Wang Y *et al* 2021 An underwater flag-like triboelectric nanogenerator for harvesting ocean current energy under extremely low velocity condition *Nano Energy* **90** 106503
- [74] Zhang H, Huang Y Z, Du X R, Yang Y Q, Li S Q, Fan D Y, Xiao X, Mutsuda H and Jiao P C 2024 Self-powered and self-sensing blue carbon ecosystems by hybrid fur

- triboelectric nanogenerators (F-TENG) *Nano Energy* **119** 109091
- [75] Wu M W, Zhu C Q, Si J C, Wang H, Xu M Y and Mi J C 2023 Recent progress in flow energy harvesting and sensing based on triboelectric nanogenerators *Adv. Mater. Technol.* **8** 2300919
- [76] Wang X Y, Chen L T, Xu Z Q, Chen P F, Ye C Y, Chen B D, Jiang T, Hong Z Y and Wang Z L 2023 High-durability stacked disc-type rolling triboelectric nanogenerators for environmental monitoring around charging buoys of unmanned ships *Small* **20** 2310809
- [77] Liang X, Liu S J, Lin S Q, Yang H B, Jiang T and Wang Z L 2023 Liquid–solid triboelectric nanogenerator arrays based on dynamic electric-double-layer for harvesting water wave energy *Adv. Energy Mater.* **13** 2300571
- [78] Hu Y C, Qiu H J, Sun Q J, Wang Z L and Xu L 2023 Wheel-structured triboelectric nanogenerators with hyperelastic networking for high-performance wave energy harvesting *Small Methods* **7** 2300582
- [79] Lian Z H *et al* 2022 A cantilever beam-based triboelectric nanogenerator as a drill pipe transverse vibration energy harvester powering intelligent exploitation system *Sensors* **22** 4287
- [80] Yu H Y *et al* 2023 High performance additional mass enhanced film structure triboelectric nanogenerator for scavenging vibration energy in broadband frequency range *Nano Energy* **107** 108182
- [81] Li X W, Zhou Y, Li Z J, Guo H Y, Gong Y, Zhang D, Zhang D, Zhang Q, Wang B and Peng Y 2023 Vortex-induced vibration triboelectric nanogenerator for energy harvesting from low-frequency water flow *Energy Convers. Manage.* **292** 117383
- [82] Feng T X, Ling D, Li C Y, Zheng W T, Zhang S C, Li C, Emel'yanov A, Pozdnyakov A S, Lu L J and Mao Y C 2024 Stretchable on-skin touchless screen sensor enabled by ionic hydrogel *Nano Res.* **17** 4462–70
- [83] Zhu P C *et al* 2024 Soft multifunctional neurological electronic skin through intrinsically stretchable synaptic transistor *Nano Res.* **17** 6550–9
- [84] Demircioglu O, Cicek M O, Doganay D, Gazaloglu G, Baykal C, Cinar S and Unalan H E 2023 Triboelectric nanogenerators for blue energy harvesting in simulated wave conditions *Nano Energy* **107** 108157
- [85] Xia K, Xu Z, Hong Y and Wang L 2023 A free-floating structure triboelectric nanogenerator based on natural wool ball for offshore wind turbine environmental monitoring *Mater. Today Sustain.* **24** 100467
- [86] Wang Y, Liu X Y, Wang Y W, Wang H, Wang H, Zhang S L, Zhao T C, Xu M Y and Wang Z L 2021 Flexible seaweed-like triboelectric nanogenerator as a wave energy harvester powering marine internet of things *ACS Nano* **15** 15700–9
- [87] Saqib Q M, Chougale M Y, Khan M U, Shaukat R A, Kim J, Bae J, Lee H W, Park J I, Kim M S and Lee B G 2021 Natural seagrass tribopositive material based spray coatable triboelectric nanogenerator *Nano Energy* **89** 106458
- [88] Wang D Y, Zhang D Z, Tang M C, Zhang H, Sun T H, Yang C Q, Mao R Y, Li K S and Wang J H 2022 Ethylene chlorotrifluoroethylene/hydrogel-based liquid–solid triboelectric nanogenerator driven self-powered MXene-based sensor system for marine environmental monitoring *Nano Energy* **100** 107509
- [89] Xu H, Wang X T, Nan Y B, Zhou H, Wu Y, Wang M X, Liu W L, Duan J Z, Huang Y L and Hou B R 2023 Flexible sponge-based nanogenerator for energy harvesting from land and water transportation *Adv. Funct. Mater.* **33** 2304723
- [90] Bemmelen J M 1907 Der hydrogel und das kristallinische hydrat des kupferoxydes *Z. Anorg. Chem.* **5** 466
- [91] Ullah F, Othman M B H, Javed F, Ahmad Z and Akil H M 2015 Classification, processing and application of hydrogels: a review *Mater. Sci. Eng. C* **57** 414–33
- [92] VahidMohammadi A, Rosen J and Gogotsi Y 2021 The world of two-dimensional carbides and nitrides (MXenes) *Science* **372** eabf1581
- [93] Davies D K 1969 Charge generation on dielectric surfaces *J. Phys. D: Appl. Phys.* **2** 1533–7
- [94] Liu S L, Tong W S, Gao C X, Liu Y L, Li X N and Zhang Y H 2023 Environmentally friendly natural materials for triboelectric nanogenerators: a review *J. Mater. Chem. A* **11** 9270–99
- [95] Pal A, Ganguly A, Wei P H, Barman S R, Chang C C and Lin Z H 2024 Construction of triboelectric series and chirality detection of amino acids using triboelectric nanogenerator *Adv. Sci.* **11** 2307266
- [96] Tao X L *et al* 2023 Large and tunable ranking shift in triboelectric series of polymers by introducing phthalazinone moieties *Small Methods* **7** 2201593
- [97] Zou H Y *et al* 2019 Quantifying the triboelectric series *Nat. Commun.* **10** 1427
- [98] Chen Q, Shang H F, Cheng B X, Lu C Z, Wang Y H, Zhang Y and Shao T M 2024 Quantifying triboelectric series of polymers based on the measurement of triboelectrification with NaCl solution *Chem. Eng. J.* **488** 150871
- [99] Yuan Z Q, Wang C F, Xi J G, Han X, Li J, Han S-T, Gao W and Pan C 2021 Spherical triboelectric nanogenerator with dense point contacts for harvesting multidirectional water wave and vibration energy *ACS Energy Lett.* **6** 2809–16
- [100] Ouyang R, Huang Y, Ye H T, Zhang Z J and Xue H 2022 Copper particles-PTFE tube based triboelectric nanogenerator for wave energy harvesting *Nano Energy* **102** 107749
- [101] Cheng P *et al* 2019 Largely enhanced triboelectric nanogenerator for efficient harvesting of water wave energy by soft contacted structure *Nano Energy* **57** 432–9
- [102] Xia K Q, Fu J M and Xu Z W 2020 Multiple-frequency high-output triboelectric nanogenerator based on a water balloon for all-weather water wave energy harvesting *Adv. Energy Mater.* **10** 2000426
- [103] Luo Y Z, Li B Y, Mo L H, Ye Z C, Shen H N, Lu Y and Li S F 2022 Nanofiber-enhanced “lucky-bag” triboelectric nanogenerator for efficient wave energy harvesting by soft-contact structure *Nanomaterials* **12** 2792
- [104] Chen H M, Wang J and Ning A F 2021 Optimization of a rolling triboelectric nanogenerator based on the nano–micro structure for ocean environmental monitoring *ACS Omega* **6** 21059–65
- [105] Chau N M, Le T H, La T T H and Bui V T 2023 Industrially compatible production of customizable honeycomb-patterned poly(vinyl chloride) using food-wrapping waste for power-boosting triboelectric nanogenerator and ocean wave energy harvester *J. Sci. Adv. Mater. Devices* **8** 100637
- [106] Lin Z M, Zhang B B, Xie Y Y, Wu Z Y, Yang J and Wang Z L 2021 Elastic-connection and soft-contact triboelectric nanogenerator with superior durability and efficiency *Adv. Funct. Mater.* **31** 2105237
- [107] Zhou Z K *et al* 2024 Enhancing the output of liquid–solid triboelectric nanogenerators through surface roughness optimization *ACS Appl. Mater. Interfaces* **16** 4763–71
- [108] Wang Y F, Guo H Y, Liao J Q, Qin Y Y, Ali A and Li C Z 2023 Solid-liquid triboelectric nanogenerator based on curvature effect for harvesting mechanical and wave energy *Chem. Eng. J.* **476** 146571
- [109] Lin Z M, Zhang B B, Guo H Y, Wu Z Y, Zou H Y, Yang J and Wang Z L 2019 Super-robust and frequency-multiplied

- triboelectric nanogenerator for efficient harvesting water and wind energy *Nano Energy* **64** 103908
- [110] Li S, Jiang J X, Zhai N N, Liu J Y, Feng K, Chen Y F, Wen Z, Sun X H and Zhong J 2022 A half-wave rectifying triboelectric nanogenerator for self-powered water splitting towards hydrogen production *Nano Energy* **93** 106870
- [111] Wu H, Wang Z K and Zi Y L 2021 Multi-mode water-tube-based triboelectric nanogenerator designed for low-frequency energy harvesting with ultrahigh volumetric charge density *Adv. Energy Mater.* **11** 2100038
- [112] Sun W X, Zheng Y B, Li T H, Feng M, Cui S W, Liu Y P, Chen S G and Wang D A 2021 Liquid-solid triboelectric nanogenerators array and its applications for wave energy harvesting and self-powered cathodic protection *Energy* **217** 119388
- [113] Wei X L, Zhao Z H, Zhang C G, Yuan W, Wu Z Y, Wang J and Wang Z L 2021 All-weather droplet-based triboelectric nanogenerator for wave energy harvesting *ACS Nano* **15** 13200–8
- [114] Dai S S, Chai Y C, Liu H X, Yu D, Wang K Y, Kong F K and Chen H L 2023 Experimental study of high performance mercury-based triboelectric nanogenerator for low-frequency wave energy harvesting *Nano Energy* **115** 108728
- [115] Zhang L M, Han C B, Jiang T, Zhou T, Li X H, Zhang C and Wang Z L 2016 Multilayer wavy-structured robust triboelectric nanogenerator for harvesting water wave energy *Nano Energy* **22** 87–94
- [116] Xu L, Pang Y K, Zhang C, Jiang T, Chen X Y, Luo J J, Tang W, Cao X and Wang Z L 2017 Integrated triboelectric nanogenerator array based on air-driven membrane structures for water wave energy harvesting *Nano Energy* **31** 351–8
- [117] Tao K *et al* 2020 Origami-inspired electret-based triboelectric generator for biomechanical and ocean wave energy harvesting *Nano Energy* **67** 104197
- [118] Tripathy R R, Sahoo R, Mishra S, Das B, Balasubramaniam S and Ramadoss A 2023 Fabrication and feasibility study of polymer-based triboelectric nanogenerator towards blue energy harvesting *Green Energy Resour.* **1** 100006
- [119] Ding Z D, Tian Z J, Ji X X, Wang D X, Ci X, Shao X J and Rojas O J 2023 Cellulose-based superhydrophobic wrinkled paper and electrospinning film as green tribolayer for water wave energy harvesting *Int. J. Biol. Macromol.* **234** 122903
- [120] Zhang C Y, Zhang W L, Du G L, Fu Q, Mo J L and Nie S X 2023 Superhydrophobic cellulosic triboelectric materials for distributed energy harvesting *Chem. Eng. J.* **452** 139259
- [121] Yang H M, Fan F R, Xi Y and Wu W Z 2020 Bio-derived natural materials based triboelectric devices for self-powered ubiquitous wearable and implantable intelligent devices *Adv. Sustain. Syst.* **4** 2000108
- [122] Su Z P, Yang Y, Huang Q B, Chen R W, Ge W J, Fang Z Q, Huang F and Wang X H 2022 Designed biomass materials for “green” electronics: a review of materials, fabrications, devices, and perspectives *Prog. Mater. Sci.* **125** 100917
- [123] Haghayegh M, Cao R, Zabihí F, Bagherzadeh R, Yang S Y and Zhu M F 2022 Recent advances in stretchable, wearable and bio-compatible triboelectric nanogenerators *J. Mater. Chem. C* **10** 11439–71
- [124] Pang Y K, Xi F B, Luo J J, Liu G X, Guo T and Zhang C 2018 An alginate film-based degradable triboelectric nanogenerator *RSC Adv.* **8** 6719–26
- [125] Wang B Q, Wu Y, Liu Y, Zheng Y B, Liu Y, Xu C G, Kong X, Feng Y G, Zhang X L and Wang D A 2020 New hydrophobic organic coating based triboelectric nanogenerator for efficient and stable hydropower harvesting *ACS Appl. Mater. Interfaces* **12** 31351–9
- [126] Zaw N Y W, Yun J, Goh T S, Kim I, Kim Y, Lee J S and Kim D 2022 All-polymer waterproof triboelectric nanogenerator towards blue energy harvesting and self-powered human motion detection *Energy* **247** 123422
- [127] Ahn J *et al* 2022 All-recyclable triboelectric nanogenerator for sustainable ocean monitoring systems *Adv. Energy Mater.* **12** 2201341
- [128] Miao X, Yang H X, Li Z K, Cheng M F, Zhao Y L, Wan L Y, Yu A F and Zhai J Y 2024 A columnar multi-layer sliding triboelectric nanogenerator for water wave energy harvesting independent of wave height and direction *Nano Res.* **17** 3029–34
- [129] Li W T, Wan L Y, Lin Y, Liu G L, Qu H, Wen H G, Ding J J, Ning H and Yao H L 2022 Synchronous nanogenerator with intermittent sliding friction self-excitation for water wave energy harvesting *Nano Energy* **95** 106994
- [130] Cai N X, Sun P and Jiang S H 2021 Rapid prototyping and customizable multifunctional structures: 3D-printing technology promotes the rapid development of TENGs *J. Mater. Chem. A* **9** 16255–80
- [131] Jing Z X, Zhang J C, Wang J L, Zhu M K, Wang X X, Cheng T H, Zhu J Y and Wang Z L 2022 3D fully-enclosed triboelectric nanogenerator with bionic fish-like structure for harvesting hydrokinetic energy *Nano Res.* **15** 5098–104
- [132] Xi F B, Pang Y K, Liu G X, Wang S W, Li W, Zhang C and Wang Z L 2019 Self-powered intelligent buoy system by water wave energy for sustainable and autonomous wireless sensing and data transmission *Nano Energy* **61** 1–9
- [133] Li Y H, Guo Z T, Zhao Z H, Gao Y K, Yang P Y, Qiao W Y, Zhou L L, Wang J and Wang Z L 2023 Multi-layered triboelectric nanogenerator incorporated with self-charge excitation for efficient water wave energy harvesting *Appl. Energy* **336** 120792
- [134] Zhong W, Xu L, Yang X D, Tang W, Shao J J, Chen B D and Wang Z L 2019 Open-book-like triboelectric nanogenerators based on low-frequency roll-swing oscillators for wave energy harvesting *Nanoscale* **11** 7199–208
- [135] Yuan W, Zhang B F, Zhang C G, Yang O, Liu Y B, He L X, Zhou L L, Zhao Z H, Wang J and Wang Z L 2022 Anaconda-shaped spiral multi-layered triboelectric nanogenerators with ultra-high space efficiency for wave energy harvesting *One Earth* **5** 1055–63
- [136] Wen H G, Yang P Y, Liu G L, Xu S X, Yao H L, Li W T, Qu H, Ding J J, Li J Y and Wan L Y 2022 Flower-like triboelectric nanogenerator for blue energy harvesting with six degrees of freedom *Nano Energy* **93** 106796
- [137] Li H H, Liang C J, Ning H, Liu J Q, Zheng C Y, Li J Y, Yao H L, Peng Y, Wan L Y and Liu G L 2022 O-ring-modularized triboelectric nanogenerator for robust blue energy harvesting in all-sea areas *Nano Energy* **103** 107812
- [138] Feng J R, Zhou H L, Cao Z, Zhang E Y, Xu S X, Li W T, Yao H L, Wan L Y and Liu G L 2022 0.5 m triboelectric nanogenerator for efficient blue energy harvesting of all-sea areas *Adv. Sci.* **9** 2204407
- [139] Yang X D, Xu L, Lin P, Zhong W, Bai Y, Luo J J, Chen J and Wang Z L 2019 Macroscopic self-assembly network of encapsulated high-performance triboelectric nanogenerators for water wave energy harvesting *Nano Energy* **60** 404–12
- [140] Liu L Q, Yang X L, Zhao L L, Hong H X, Cui H, Duan J L, Yang Q M and Tang Q W 2021 Nodding duck structure multi-track directional freestanding triboelectric

- nanogenerator toward low-frequency ocean wave energy harvesting *ACS Nano* **15** 9412–21
- [141] Wang H, Zhu C Q, Wang W C, Xu R J, Chen P E, Du T L, Xue T X, Wang Z Y and Xu M Y 2022 A stackable triboelectric nanogenerator for wave-driven marine buoys *Nanomaterials* **12** 594
- [142] Ying Q Y, Wu J Y and Liu C 2024 Multi-track triboelectric nanogenerator toward omnidirectional ocean wave energy harvesting *Adv. Mater. Technol.* **9** 2301824
- [143] Duan Y X, Xu H X, Liu S J, Chen P F, Wang X Y, Xu L, Jiang T and Wang Z L 2023 Scalable rolling-structured triboelectric nanogenerator with high power density for water wave energy harvesting toward marine environmental monitoring *Nano Res.* **16** 11646–52
- [144] Xiao T X, Liang X, Jiang T, Xu L, Shao J J, Nie J H, Bai Y, Zhong W and Wang Z L 2018 Spherical triboelectric nanogenerators based on spring-assisted multilayered structure for efficient water wave energy harvesting *Adv. Funct. Mater.* **28** 1802634
- [145] Lei R, Zhai H, Nie J H, Zhong W, Bai Y, Liang X, Xu L, Jiang T, Chen X Y and Wang Z L 2019 Butterfly-inspired triboelectric nanogenerators with spring-assisted linkage structure for water wave energy harvesting *Adv. Mater. Technol.* **4** 1800514
- [146] Liang X, Jiang T, Liu G X, Feng Y W, Zhang C and Wang Z L 2020 Spherical triboelectric nanogenerator integrated with power management module for harvesting multidirectional water wave energy *Energy Environ. Sci.* **13** 277–85
- [147] Liang X, Liu Z R, Feng Y W, Han J J, Li L L, An J, Chen P F, Jiang T and Wang Z L 2021 Spherical triboelectric nanogenerator based on spring-assisted swing structure for effective water wave energy harvesting *Nano Energy* **83** 105836
- [148] Wang A Q, Chen J, Wang L, Han J L, Su W G, Li A Q, Liu P B, Duan L Y, Xu C H and Zeng Z 2022 Numerical analysis and experimental study of an ocean wave tetrahedral triboelectric nanogenerator *Appl. Energy* **307** 118174
- [149] Liang X, Liu S J, Ren Z W, Jiang T and Wang Z L 2022 Self-powered intelligent buoy based on triboelectric nanogenerator for water level alarming *Adv. Funct. Mater.* **32** 2205313
- [150] Liu S J, Liang X, Chen P F, Long H R, Jiang T and Wang Z L 2023 Multilayered helical spherical triboelectric nanogenerator with charge shuttling for water wave energy harvesting *Small Methods* **7** 2201392
- [151] Jung H, Ouro-Koura H, Salalila A, Salalila M and Deng Z D 2022 Frequency-multiplied cylindrical triboelectric nanogenerator for harvesting low frequency wave energy to power ocean observation system *Nano Energy* **99** 107365
- [152] Yang Y H, Zheng L, Wen J, Xing F J, Liu H, Shang Y R, Wang Z L and Chen B 2023 A swing self-regulated triboelectric nanogenerator for high-entropy ocean breaking waves energy harvesting *Adv. Funct. Mater.* **33** 2304366
- [153] Gao Q, Xu Y H, Yu X, Jing Z X, Cheng T H and Wang Z L 2022 Gyroscope-structured triboelectric nanogenerator for harvesting multidirectional ocean wave energy *ACS Nano* **16** 6781–8
- [154] Feng Y W, Jiang T, Liang X, An J and Wang Z L 2020 Cylindrical triboelectric nanogenerator based on swing structure for efficient harvesting of ultra-low-frequency water wave energy *Appl. Phys. Rev.* **7** 021401
- [155] Wang J L, Li Y K, Xie Z J, Xu Y H, Zhou J W, Cheng T H, Zhao H W and Wang Z L 2020 Cylindrical direct-current triboelectric nanogenerator with constant output current *Adv. Energy Mater.* **10** 1904227
- [156] Yang Y H, Wen J, Chen F R, Hao Y T, Gao X B, Jiang T, Chen B D and Wang Z L 2022 Barycenter self-adapting triboelectric nanogenerator for sea water wave high-entropy energy harvesting and self-powered forecasting in marine meteorology *Adv. Funct. Mater.* **32** 2200521
- [157] Jiang W Y, Chen C J, Wang C Y, Li J W, Zhao M M, Xiang T F and Wang P 2023 Design of triboelectric nanogenerators featuring motion form conversion, motion rectification, and frequency multiplication for low-frequency ocean energy harvesting *Energy Environ. Sci.* **16** 6003–14
- [158] Qiu H J, Wang H M, Xu L, Zheng M L and Wang Z L 2023 Brownian motor inspired monodirectional continuous spinning triboelectric nanogenerators for extracting energy from irregular gentle water waves *Energy Environ. Sci.* **16** 473–83
- [159] Zhang C G, Yuan W, Zhang B F, Yang J Y, Hu Y X, He L X, Zhao X J, Li X H, Wang Z L and Wang J 2023 A rotating triboelectric nanogenerator driven by bidirectional swing for water wave energy harvesting *Small* **19** 2304412
- [160] Han J J, Liu Y, Feng Y W, Jiang T and Wang Z L 2023 Achieving a large driving force on triboelectric nanogenerator by wave-driven linkage mechanism for harvesting blue energy toward marine environment monitoring *Adv. Energy Mater.* **13** 2203219
- [161] Jiang T, Pang H, An J, Lu P J, Feng Y W, Liang X, Zhong W and Wang Z L 2020 Robust swing-structured triboelectric nanogenerator for efficient blue energy harvesting *Adv. Energy Mater.* **10** 2000064
- [162] Tan D J, Zeng Q X, Wang X, Yuan S L, Luo Y L, Zhang X F, Tan L M, Hu C G and Liu G L 2022 Anti-overturning fully symmetrical triboelectric nanogenerator based on an elliptic cylindrical structure for all-weather blue energy harvesting *Nano-Micro Lett.* **14** 124
- [163] Xu L, Jiang T, Lin P, Shao J J, He C, Zhong W, Chen X Y and Wang Z L 2018 Coupled triboelectric nanogenerator networks for efficient water wave energy harvesting *ACS Nano* **12** 1849–58
- [164] Liu W B, Xu L, Liu G X, Yang H, Bu T Z, Fu X P, Xu S H, Fang C L and Zhang C 2020 Network topology optimization of triboelectric nanogenerators for effectively harvesting ocean wave energy *iScience* **23** 101848
- [165] Liu G L, Xiao L F, Chen C Y, Liu W L, Pu X J, Wu Z Y, Hu C G and Wang Z L 2020 Power cables for triboelectric nanogenerator networks for large-scale blue energy harvesting *Nano Energy* **75** 104975
- [166] Li X Y, Xu L, Lin P, Yang X D, Wang H M, Qin H F and Wang Z L 2023 Three-dimensional chiral networks of triboelectric nanogenerators inspired by metamaterial's structure *Energy Environ. Sci.* **16** 3040–52
- [167] Zhu Z Y, Xiang H J, Zeng Y M, Zhu J Q, Cao X, Wang N and Wang Z L 2022 Continuously harvesting energy from water and wind by pulsed triboelectric nanogenerator for self-powered seawater electrolysis *Nano Energy* **93** 106776
- [168] Leung S F, Fu H C, Zhang M L, Hassan A H, Jiang T, Salama K N, Wang Z L and He J H 2020 Blue energy fuels: converting ocean wave energy to carbon-based liquid fuels via CO₂ reduction *Energy Environ. Sci.* **13** 1300–8
- [169] Hou C, Chen T, Li Y F, Huang M J, Shi Q F, Liu H C, Sun L N and Lee C 2019 A rotational pendulum based electromagnetic/triboelectric hybrid-generator for ultra-low-frequency vibrations aiming at human motion and blue energy applications *Nano Energy* **63** 103871
- [170] Zhang X Q *et al* 2019 Self-powered distributed water level sensors based on liquid-solid triboelectric nanogenerators for ship draft detecting *Adv. Funct. Mater.* **29** 1900327

- [171] Shan C C *et al* 2023 Dual mode TENG with self-voltage multiplying circuit for blue energy harvesting and water wave monitoring *Adv. Funct. Mater.* **33** 2305768
- [172] Liu H Y, Xiao Y, Xu Y, Zhang S C, Qu C M and Zhang Y L 2023 A highly adaptive real-time water wave sensing array for marine applications *Nanoscale* **15** 9162–70
- [173] Liu L, Shi Q F, Ho J S and Lee C 2019 Study of thin film blue energy harvester based on triboelectric nanogenerator and seashore IoT applications *Nano Energy* **66** 104167
- [174] Liu L, Shi Q F and Lee C 2020 A novel hybridized blue energy harvester aiming at all-weather IoT applications *Nano Energy* **76** 105052
- [175] Bai Y, Xu L, He C, Zhu L P, Yang X D, Jiang T, Nie J H, Zhong W and Wang Z L 2019 High-performance triboelectric nanogenerators for self-powered, in-situ and real-time water quality mapping *Nano Energy* **66** 104117
- [176] Shi Q F, Wang H, Wu H and Lee C 2017 Self-powered triboelectric nanogenerator buoy ball for applications ranging from environment monitoring to water wave energy farm *Nano Energy* **40** 203–13
- [177] Liu J H *et al* 2024 Underwater biomimetic lateral line sensor based on triboelectric nanogenerator for dynamic pressure monitoring and trajectory perception *Small* **20** 2308491
- [178] Zhao D, Li H Y, Wang J L, Gao Q, Yu Y, Wen J M, Wang Z L and Cheng T H 2023 A drawstring triboelectric nanogenerator with modular electrodes for harvesting wave energy *Nano Res.* **16** 10931–7
- [179] Zhao D, Li H Y, Yu Y, Wang Y T, Wang J L, Gao Q, Wang Z L, Wen J M and Cheng T H 2023 A current-enhanced triboelectric nanogenerator with crossed rollers for harvesting wave energy *Nano Energy* **117** 108885
- [180] Chandrasekhar A, Vivekananthan V, Khandelwal G and Kim S J 2020 A sustainable blue energy scavenging smart buoy toward self-powered smart fishing net tracker *ACS Sustain. Chem. Eng.* **8** 4120–7
- [181] Li X Y, Tao J, Wang X D, Zhu J, Pan C F and Wang Z L 2018 Networks of high performance triboelectric nanogenerators based on liquid–solid interface contact electrification for harvesting low-frequency blue energy *Adv. Energy Mater.* **8** 1800705
- [182] Zhao X J, Tian J J, Kuang S Y, Ouyang H, Yan L, Wang Z L, Li Z and Zhu G 2016 Biocide-free antifouling on insulating surface by wave-driven triboelectrification-induced potential oscillation *Adv. Mater. Interfaces* **3** 1600187
- [183] Wang X Y, Ye C Y, Chen P F, Pang H, Wei C H, Duan Y X, Jiang T and Wang Z L 2024 Achieving high power density and durability of multilayered swing-structured triboelectric nanogenerator toward marine environmental protection *Adv. Funct. Mater.* **34** 2311196
- [184] Mo J L, Liu Y H, Fu Q, Cai C C, Lu Y X, Wu W H, Zhao Z X, Song H N, Wang S F and Nie S X 2022 Triboelectric nanogenerators for enhanced degradation of antibiotics via external electric field *Nano Energy* **93** 106842
- [185] Xu G Q, Li X Y, Fu J J, Zhou Y K, Xia X and Zi Y L 2023 Environmental lifecycle assessment of CO₂-filled triboelectric nanogenerators to help achieve carbon neutrality *Energy Environ. Sci.* **16** 2112–9
- [186] Ahmed A, Wang Y N, Azam A, Li N, Jia C Y and Zhang Z T 2023 Design of an S-shaped point-absorber wave energy converter with a non-linear PTO to power the satellite-respondent buoys in the East China Sea *Ocean Eng.* **275** 114162
- [187] Zhang Y K, Wen Y, Han X Y, Zhang W D, Gao F and Chen W X 2023 Gyroscopic wave energy converter with a self-accelerating rotor in WEC-glider *Ocean Eng.* **273** 113819
- [188] Ding W J, Song B W, Mao Z Y and Wang K Y 2016 Experimental investigations on a low frequency horizontal pendulum ocean kinetic energy harvester for underwater mooring platforms *J. Mar. Sci. Technol.* **21** 359–67
- [189] Chen W X, Lu Y F, Li S X and Gao F 2023 A bio-inspired foldable-wing wave energy converter for ocean robots *Appl. Energy* **334** 120696
- [190] Jia C Y, Cao H, Pan H Y, Ahmed A, Jiang Z J, Azam A, Zhang Z T and Pan Y J 2022 A wave energy converter based on a zero-pressure-angle mechanism for self-powered applications in near-zero energy sea-crossing bridges *Smart Mater. Struct.* **31** 095006
- [191] Liang C W, Ai J X and Zuo L 2017 Design, fabrication, simulation and testing of an ocean wave energy converter with mechanical motion rectifier *Ocean Eng.* **136** 190–200
- [192] Binh P C, Tri N M, Dung D T, Ahn K K, Kim S J and Koo W 2016 Analysis, design and experiment investigation of a novel wave energy converter *IET Gen. Transm. Distrib.* **10** 460–9